ACS OMEGA

http://pubs.acs.org/journal/acsodf

Article

Ultralow Sulfur Diesel and Rapeseed Methyl Ester Fuel Impact on Performance, Emitted Regulated, Unregulated, and Nanoparticle Pollutants

Miqdam T Chaichan,* Mohammed A. Fayad, Amged Al Ezzi, Hayder A Dhahad, T. Megaritis, Talal Yusaf, Ahmed Al-Amiery,* and Wan Nor Roslam Wan Isahak

Cite This: *ACS Omega* 2022, 7, 26056−26075

Read Online

ACCESS | Metrics & More | Article Recommendations

ABSTRACT: The operation of engines using rapeseed methyl ester (RME) and ultralow sulfur diesel (ULSD) was tested for the combustion properties, emitted regulated, unregulated exhaust pollutants, and the size of nanoparticles. The combustion analysis showed higher apparent heat release rate and shorter ignition delay period during RME combustion than during ULSD combustion. The ULSD engine has a combustion chamber maximum pressure relatively higher than that of RME. This study showed that the heat release rate of ULSD is always higher than that of RME while more fuel consumption occurred from the combustion of biodiesel in comparison with diesel. When the engine is running on RME, HC and NOx formation increased at high loads up to 15% and 13%, respectively; meanwhile, CO concentrations reduced by 30.9% for the same conditions. Most of the particulate matter (PM) emitted from a diesel engine has a particle size from 5 to 100 nm, while the particle size from ULSD ranged from 5 to 40 nm. Overloading the engine caused a decrease in the sizes of emitted PM for both fuels. The smoke number for RME was less than that for ULSD by 33.9% at high loads. For high engine load, the cumulative concentration number for the nucleation mode decreased, while it increased for the accumulation mode. Furthermore, measurements of formaldehyde, ethane, methane, acetylene, ethylene, propylene, and isocyanic acid emissions showed the presence of these harmful substances at very low concentrations (8 ppm) for both fuels.

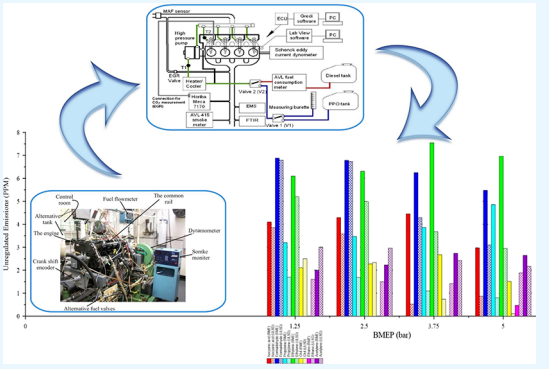

1. INTRODUCTION

Due to the steady increase in population around the world, the rise in the standard of living, and the total dependence on transportation vehicles mostly powered by fossil fuels, the world's fossil fuel reserves are experiencing a sharp decline. Diesel (a derivative of petroleum fuels) can be considered the most widely used in the world in the operation of vehicles, trains, ships, and electric power plants.[1] The International Energy Agency (IEA) expected that all kinds of global energy would escalate by 50% from 2005 to 2030, with the dominance of fossil fuels completely on the global energy market.[2] This huge dependence on diesel in all sectors of industrial, agricultural, and transportation sectors, which makes it the most influential fuel in the global economy, came as a result of the high reliability, durability, and high efficiency of diesel engines. What confuses this picture is that a large and substantial portion of greenhouse gases is emitted from diesel engine exhaust.[3] Diesel engines emit harmful gases that affect the health and environment such as CO and CO_2, NO_X, HC, and smoke, which are called regulated emissions. In addition, there are other types of carcinogenic and dangerous gases such as acetaldehyde, acetylene, methane, ethylene, and propylene that are called unregulated emissions. The unregulated contaminants are very harmful to health and sometimes even deadly.[4,5]

Diesel combustion in compression ignition (CI) engines emits a complex mixture of gaseous emissions in addition to flammable nanoscale particles such as PM1 and PM2.5. Regular pollutants include NO_X, SO_2, HC, CO, and CO_2. As for the particulate matter (PM), it is composed of organic carbon and elementary carbon.[6,7] Generally, it can be considered that diesel engine exhaust pollutants have serious negative public health consequences as it reduces visibility and

Received: February 14, 2022
Accepted: June 16, 2022
Published: July 18, 2022

Table 1. Some Recent Studies Used Biodiesel Addition to Diesel from the Literature

ref. no.	biodiesel origin	engine used	operation conditions	brake thermal eff.	bsfc	NOx	CO	HC	PM	unregulated emissions
36	pine oil	SC, water cooled DI diesel engine (Kirloskar AV1)	constant engine speed (15 rpm) variable loads (20, 40, 60, 80, and 100%)	1.3% less than diesel	6.2% less than diesel	13.11% more than diesel	7.5% less than diesel	21% more than diesel	35.5% more than diesel	nil
37	1st generation (coconut, palm, rapeseed, soybean), 2nd generation (cottonseed, *Jatropha curcas*, jojoba, karanja), and 3rd generation (fish oil, spirulina, waste cooking oil, animal fats) feedstocks	diesel engine with a rated power of 3.5 kW at 1500 rpm	three compression ratios (16.5, 17.5, and 18.5:1) and variable loads (25, 50, 75, and 100%)	0.63% less than diesel	4% more than diesel	39.6%			51.8%	nil
38	fatty acid methyl esters	4-cylinder diesel engine-type 1.6 HDI	varying biodiesel portions in the blend by 10, 30, and 50%.	0.78% more than diesel		8% more than diesel	3.29% more than diesel	10.4% more than diesel	16.85% less than diesel	nil
39	rice bran oil and karanja oil	single-cylinder, 4-stroke, naturally aspired, DI diesel engine	diesel (D), hydrogen-enriched diesel, hydrogen-enriched 10 and 20% rice bran biodiesel, and hydrogen-enriched 10 and 20% karanja biodiesel blend	2.5% more than diesel	2.9% less than diesel	6−13% more than diesel	4−38% less than diesel	6−14% less than diesel		nil
40	waste cooking oil	4-cylinder, 4r-stroke, water-cooled, 1.461-L, turbocharged CI engine	fixed engine speed 1750 rpm and variable loads (20, 40, 60, and 80 Nm); hydrogen added by 10, 20, 30, and 40 lpm		11.1% less than diesel	2.22% more than diesel		4.27% less than diesel	65.6% less than diesel	nil
41	rapeseed oil + distilled tire pyrolytic oil	medium-duty compression-ignition engine manufactured by Andoria-Mot Poland		1.2% less than diesel		17.5% more than diesel	27.65% more than diesel	78.57% more than diesel	35% less than diesel	nil
42	*Chlorella emersonii* methyl ester (CEME) blended with diesel at 10%, 20%, 30%, 40%, and 100%	single cylinder, 4-stroke air-cooled diesel-powered Kirloskar engine (model: TAF-1)	constant speed 1500 rpm	7.7% less than diesel	7.24% more than diesel	13.6% more than diesel	8% less than diesel	16.66% less than diesel	20.54% less than diesel	toluene: 55% less than diesel; acetaldehyde: 8% more than diesel; acetone: 94% more than diesel; formaldehyde: 45% more than diesel
43	rapeseed oil methyl ester and rapeseed oil ethyl ester	4-stroke Yanmar diesel engine TF70V-E	variable speeds: 1000, 2000, and 3000 rpm		11.11% less than diesel	26.3% less than diesel	13.47% more than diesel			nil
44	methyl oleate (MO) to palm oil methyl ester (PME)	single-cylinder direct-injection Yanmar model L48N diesel engine	part load conditions (50%); constant speed 3000 rpm	4.9% less than diesel	21.04% more than diesel	14.4% more than diesel	78.3% less than diesel	68.4% less than diesel		nil
45	waste cooking oil + ethanol/octanol	single-cylinder, vertical, 4-stroke, air-cooled, DI 170 F CI diesel engine		23.77% less than diesel	33.6% more than diesel	5.45% more than diesel	8.5% less than diesel	12.7% more than diesel	-	nil
15	less than diesel	DI, 4-cylinder, Puma diesel engine	variable IT conditions (before and after TDC), 1500 rpm, and two BMEP			7% more than diesel	21% less than diesel	31% less than diesel	23% less than diesel	nil
46	preheated *Vateria indica* methyl ester (VIME)	4-stroke, single-cylinder TV1 Kirloskar diesel engine	blends (B0, B30, ,B50, and B100) with variable loads (20, 40, 60, 80, and 100%)	7.44% more than diesel	26.73% less than diesel	21.62% more than diesel	28.08% less than diesel	42.7% less than diesel	17.3% less than diesel	nil

https://doi.org/10.1021/acsomega.2c00893
ACS Omega 2022, 7, 26056−26075

Table 1. continued

ref. no.	biodiesel origin	engine used	operation conditions	brake thermal eff.	bsfc	NOx	CO	HC	PM	unregulated emissions
47	Chlamydomonas alga biodiesel	4-cylinder OM 924 diesel engine				5.58% more than diesel	0.28% less than diesel	67% less than diesel	42% less than diesel	nil
48	biodiesel + ethanol + *n*-pentanol	single-cylinder diesel engine with a common rail fuel injection system, which is 4-valve, four-stroke, and water-cooled	fixed injection timing 4° bTDC and fixed injection quantity	3% more than diesel		30.9 less than diesel	40.8% less than diesel	72% less than diesel	48% less than diesel	nil
49	*Chlorella protothecoides* biomass and rapeseed oil	single cylinder, water-cooled compression–ignition diesel engine (Kirloskar AV1)				34% less than diesel	5.2% less than diesel	33.3% less than diesel	27.27% less than diesel	nil
50	rapeseed oil–methanol–iso-butanol blends	4-cylinder turbocharged Zetor 1204 diesel engine	diesel/rapeseed oil/methanol/iso-butanol 60/30/5/5, 50/30/10/10, and 50/10/20/20	5.5 less	9.8% more	21.9% more	41.9% more		80.62% less than diesel	HCHO emissions: 77.79% more than diesel; butadiene (C_4H_6): 37.31% more than diesel; methane (CH_4): 15.97% more than diesel
51	rapeseed methyl ester (RME)-based biodiesel and rapeseed oil (RO), blended with diesel (D) and isopropanol (P)	4-cylinder turbocharged direct injection diesel engine	7 different blends prepare and tested	5% more than diesel	11% more than diesel	4% less than diesel		30% more than diesel	5% less than diesel	nil
52	waste cooking oil	2-cylinder, water cooled, Simpons S217 diesel engine	variable loads (25, 59, 75, and 100%), IT = 24° bTDC	9.7% less than diesel	25% more than diesel	13.46% more than diesel	30% less than diesel	17% less than diesel	14.08% less than diesel	nil
53	waste cooking oil	4-cylinder, common-rail diesel	the ESC (European Stationary Cycle) used in analyzing the fuel blend impact on the exhaust pollutants	1.57% more than diesel	11.02% more than diesel	17% more	3.7% less	33.9% less	53.8% less	formaldehyde: 25% more than diesel; acetaldehyde: 47.1% more than diesel; 1,3-butadiene: 109.1% more than diesel; propene: 85.36% more than diesel; ethane: 63.15% more than diesel
54	olive mill wastewater (OMWW)	single-cylinder DI, LISTER-PETTER diesel engine	IT = 13° bTDC, 1500 rpm, variable loads (25, 50, 75, and 100%)	2% less than diesel	14% more than diesel	16.6% less than diesel	26% less than diesel	12% less than diesel	12% less than diesel	nil
55	waste cooking oil and diglyme	4-cylinder DI Isuzu 4HF1 diesel engine	2400 rpm, 5-engine loads, and oxygen concentrations of 2, 4, 6, 8, and 10%	1.7% more than diesel	9.5% more than diesel				44.7% less than diesel	nil
56	waste tires pyrolysis oil (TPO) and neat palm biodiesel	turbocharged DI Renault Kangoo K9K 700 diesel engine	engine speed from 1000 to 3500 rpm and full load	3.3% more than diesel		4% less than diesel	41.6%	5.79% more than diesel	20.2% less than diesel	nil
57	*V. indica* methyl ester (VIME	single-cylinder, TV1 Kirloskar DI diesel engine		0.6% more than diesel	26.27% more than diesel	36.19% more than diesel	16.2% less than diesel	34.4% less than diesel	16.5% less than diesel	nil
58	partially hydrogenated biodiesel (PHB)–ethanol–diesel ternary blend	turbocharged, 4-cylinder common rail diesel engine	various loads and 1800 rpm		4.7% more than diesel	100% more than diesel	45.45 more than diesel	62.5% less than diesel	60.86% less than diesel	SO_2: 28% less than diesel; HCHO: 50% more than diesel; C_2H_4: 29.41% less than diesel; AHC: 31.8% less than diesel

https://doi.org/10.1021/acsomega.2c00893
ACS Omega 2022, 7, 26056−26075

http://pubs.acs.org/journal/acsodf

Table 1. continued

ref. no.	biodiesel origin	engine used	operation conditions	brake thermal eff.	bsfc	NOx	CO	HC	PM	unregulated emissions
59	cottonseed and palm oil biodiesels	single-cylinder, 4-stroke, and the natural aspiration diesel engine	variable engine speed from 1400 to 2400 rpm; 100% engine load	9.5% less than diesel	10.4% more than diesel	26.5% more than diesel	18.9% less than diesel	29.04% less than diesel	26.05% less than diesel	
60	*C. pyrenoidosa* microalgae biodiesel (CP20D80)	single-cylinder, water-cooled light commercial CI engine	PIT (pilot injection timing) of 20° aTDC and 15° aTDC and maximum load condition	3.7% more than diesel	2.7% less than diesel	37.5% more than diesel	65.2% less than diesel	67.25% less than diesel	67.85% less than diesel	
61	coconut, sunflower, and palm oils	single-cylinder, water-cooled DI diesel engine	9 blends tested at constant speed and variable load	0.52% less than diesel	5.3% more than diesel		95% less than diesel	23.5% less than diesel	4.5% less than diesel	
62	diethyl ether (DEE)	3-cylinder, water-cooled, DI tractor diesel engine	1500 rpm and variable engine loads			33.33% less than diesel				*n*-pentane (n-C_5H_{12}): 150% more than diesel; *n*-octane (n-C_8H_{18}): 170% more than diesel; iso-butene (iso-C_4H_8): 58.8% more than diesel; formic acid (HCOOH): 50% more than diesel; formaldehyde (HCHO): 92.85% more than diesel
63	85% light hydrocarbon (LHC)-diesel blends	six-cylinder (Z6170ZLCZ-19) diesel engine	1000 rpm and variable loads (50, 75, and 100%)			38.09% less than diesel	17.6% less than diesel	80% more than diesel		OSC: 20.48% more than diesel; BRCS: 483% more than diesel; NAHC: 253% more than diesel
64	coconut oil-diesel fuel blends	4-cylinder, turbocharged diesel engine	variable loads (25, 50, 75, and 100%); variable speed (1600, 2350, 3100, and 3850 rpm)	0.84% less than diesel	2.44% more than diesel	11.93% more than diesel	12.9% less than diesel		14.79% less than diesel	nil

https://doi.org/10.1021/acsomega.2c00893
ACS Omega 2022, 7, 26056−26075

causes acid rain in addition to its major role in global climate change.[8,9]

The rate of emission of any of the abovementioned pollutants depends on many overlapping variables and the sampling conditions. The most important of these variables are engine type, combustion chamber type,[10] injection method and injection angle, engine operating method,[11] and fuel type in addition to the after-treatment method used.[12] Many countries around the world have set strict standards on emissions of exhaust gases from diesel engines. The manufacturers of these engines have also tended to develop advanced technologies for controlling engine emissions. The global research trend in the study of diesel engines works in two basic directions, namely, to reduce both specific fuel consumption (SFC) and exhaust gas pollutants to meet the standards imposed by the United States of America and the European Union.

New ignition methods are among the many options presented in this direction, and HCCI,[13,14] PPCI,[15,16] and LTC engines have emerged.[17,18] Several researchers have also added small proportions of variable types of nanoadditives to the diesel fuel in order to improve combustion characteristics and reduce pollutants.[19,20] Some important studies mixed diesel fuel with water to form an emulsion that takes advantage of hydrogen and aqueous oxygen atoms in the combustion.[21,22] Since the nineties of the last century until today, studies are continuing to add many types of biofuels to diesel because this fuel is produced from natural sources as it is an oxygenator that contains in its chemical composition oxygen that improves the combustion process inside the combustion chamber.[23,24]

Among biofuel types, biodiesel is a very promising renewable fuel. Biodiesels can feed diesel engines without any engine modifications.[25,26] Biodiesels consist of long chain fatty acid monoalkyl esters that are derived from animal fats, vegetable oils, and yellow grease. Biodiesel is sulfur-free, renewable, nontoxic, high-oxygen, and biodegradable. It has an energy density comparable to that of fossil diesel. The cetane number is less in biodiesel properties than that of diesel fuel, but it is rather close and has a high percentage of oxygen in its chemical composition.[27,28] Against this beautiful picture, biodiesel is characterized by high viscosity, high molecular weight, and low volatility, and these properties cause several problems such as high sedimentation rate in the combustion chamber that causes the injector to close and stick to the piston ring.[29] Moreover, diesel−biodiesel mixtures are considered unsuitable for use in cold weathers due to phase separation, which results in equipping the engine with a heterogeneous mixture of fuel.[30] In general, replacing diesel with biodiesel can contribute to significant reduction in carbon monoxide, sulfur dioxide, volatile organic compounds, hydrocarbons, and PM emitted. However, most experimental studies confirm that the levels of NO_X emissions increase.[31−33] The switch to biofuels produced from agricultural crops can be seen as a threat to global food security. Hence, most researchers in this field have adopted the use of biofuels that come from waste cooking oil from restaurants and home kitchens, but these sources are not permanent and are not a continuous supply.[34] Biodiesel produced from animal fats such as inedible beef, duck fat, fish fat, and yellow fats as waste from manufacturing processes can be considered as a permanent source for preparing the raw materials for biodiesel at lower cost.[35]

Table 1 lists some recent studies that investigated the addition of many types of biofuels to diesel and the resulting effect on engine performance and emissions.

In diesel engines, the internal combustion is characterized by the controlled mixing of air−fuel inside the engine cylinders. Diesel engines emit high levels of NO_X and smoke.[65,66] The bulk of the soot is formed during the combustion period, which is controlled by mixing. In the late combustion stage, most of the soot formed is oxidized. As for NO_X, it forms at high temperatures in the flame front. Exhaust gas recycling (EGR) technology is considered one of the most effective methods of reducing NO_X concentrations by reducing the flame temperature. Studies have proven that an increase in EGR rates causes a rise in PM concentrations due to a decrease in oxygen concentration in the combustion chamber, which causes disruption of soot oxidation. From here, it was found that the oxygen present in the biodiesel will solve part of this dilemma and reduce the PM concentrations, although it will cause a limited rise in the NO_X concentrations. Working with a high engine injection pressure will reduce PM concentrations, but NO_X levels will increase. Finding a way to reduce both NO_X and PM levels to fulfill stringent emission legislations can be considered a complex and difficult task.[65,67]

The researchers examined several options in diesel engines to solve this issue. Moniru et al.[68] added palm and Jatropha oils to diesel at rates of 10% and 20% and found that fuel consumption increased by 7.96% to 10.15%, respectively. The study showed that adding 10% Jatropha to diesel caused smoke opacity to decrease by 31.09% compared to diesel. Chaichan[69] studied the possibility of utilizing hydrogen entering into the combustion chamber through the intake manifold with the use of diesel−biodiesel and the recycling of cold and hot exhaust gas. The addition of hydrogen raised the temperatures inside the combustion chamber that increased the NO_X levels in the exhaust gas, while the use of EGR at high levels caused a decrease in the brake thermal efficiency. The researcher found the possibility of reducing NO_X levels by adopting the percentages of hydrogen and EGR at a specific additive. Additionally, the used technique caused a decrease in PM levels but increased engine noise.

Some researchers have adopted the multiple injection method of diesel−biodiesel mixtures to achieve low NO_X and PM levels. For example, Naresh Kumar et al.[70] used an 80% diesel−20% palm oil methyl ester blend with a multiple fuel injection engine running. The injection was divided into 10%, 20%, and 30%, with two injection angles of 33° bTDC and 23° bTDC. The researchers claimed superior performance while NO_X levels increased by 7.19% compared to pure diesel. Karthic et al.[71] added *Syzygium cumini* oil in various proportions (30%, 70%, and 100%) to diesel fuel and studied the effect of changing the engine injection timing (21°, 23°, and 25° CA bTDC) and the injection pressure (200, 220, 240, and 260 bar) on the engine's performance and contaminants. They concluded that the engine performance was significantly enhanced by advancing the injection timing by 2° CA bTDC and raising the fuel injection pressure to 240 bar. B30 (70% diesel−30% biodiesel blend) gave the best engine performance under these operating conditions. Also, the levels of CO and HC were reduced by 15.9% and 46.15%, respectively. Engine operation at advanced injection timing and high fuel injection pressure caused reduction in the smoke level by about 28.7%. However, under these operating conditions, NO_X levels were increased.

https://doi.org/10.1021/acsomega.2c00893
ACS Omega 2022, 7, 26056−26075

Ashok et al.[72] used a pilot injection of 10% and injection pressures of 400, 500, and 600 bar to operate an engine (type CRDI) fueled with biodiesel produced from natural lemon peel oil that had a low viscosity. The researchers also increased the pilot injection rate to 20% and 30% at a constant injection pressure of 600 bar. The last case studied was when 10% exhaust gas recirculating (EGR) was introduced at a pilot injection of 30%. The study concluded that the fuel−air mixing is better at high injection pressures, resulting in an increase in the bsfc. The fuel consumption was reduced while NO_X concentrations were increased by 13.6% at engine operation with high combustion rates during the ignition-lag period. The study recommended adding approximately 20% or 30% EGR to the combustion chamber to reduce NO_X levels.

Heywood[73] studied the effect of adding antioxidants such as aromatic amines (DPPD, PPD) and phenols (BHT, BHA) on the NO_X and smoke levels emitted from an engine powered by diesel−biodiesel (produced from sunflower) blends. Compared to diesel fuel, the engine operation with the studied blends caused a slight increase in bsfc but enhanced the brake thermal efficiency. The addition of PPD caused a decrease of 52% in NO_X concentrations compared to the other antioxidants.

As shown in the above literature survey and Table 1, for most of the studies, measuring the emitted unregulated pollutants has been neglected, despite the fact that these pollutants are the most toxic and dangerous to public health. The reason may be due to the difficulty of measuring them or considering their concentrations to be very small compared to pollutants such as CO, HC, and NO_X. However, these small values, when produced by millions of operating engines, will have very serious toxic effects and must be treated as the case of the regulated pollutants. Therefore, in this study, a high-speed direct injection diesel engine (HSDI) fueled with ultralow sulfur diesel and rapeseed biodiesel (RME) blends is used. To reduce the NO_X and PM together, the tests were conducted under constant engine speed conditions (1500 rpm) and variable loads (four loads). A constant fuel injection pressure (800 bar) and injection timing (9° bTDC) were also used. The study aims to investigate the impact of the above engine operating parameters on the levels of regulated, unregulated, and nanoparticle emissions of the engine. The study will show conclusively that biodiesel reduces some of the regulated pollutants, but it increases the unregulated ones compared to the diesel. Therefore, serious consideration must be given to setting limits to unregulated pollutants to ensure the safety of public health and the environment.

2. MATERIALS AND METHODS

2.1. Test Fuels. The diesel fuel used in the study is an ultralow sulfur diesel (ULSD) fuel manufactured by the Shell Company. Also, pure rapeseed methyl ester (RME) produced by the Shell Company in the UK, which is famous for the cultivation of rapeseed, was used. The production of biodiesel from rapeseed is a mature technology, but the production costs are high and are twice the price of non-taxable diesel fuel. Perhaps the bulk of the price is due to the fact that only 41% of the dry biomass weight is oil. Table 2 lists the used fuels' properties, which were supplied by the manufacturing companies.

Table 2 shows that the number of carbon atoms in biodiesel is more than its counterparts in diesel while the cetane number is relatively higher and also the viscosity and density are much higher than the case of the diesel used. The height of the last two traits has a negative effect on the injection process as it requires higher pressures, but in this study, the used engine has a high injection pressure (800 bar), which means that these two properties will not affect the injection process. However, they will have an effect on the process of evaporation and mixing with air. Biodiesel contains 10.84% oxygen in its composition. This amount will help improve combustion and reduce pollutants. Low-sulfur diesel fuel contains 46 mg/kg oxygen, which is a low quantity, and it will limit the formation of sulfur oxides that poison catalysts. Also, a higher decrease in sulfur will reduce the formation of particulate matter. The calorific value of the biodiesel is significantly lower than the calorific value of diesel. The lower calorific value means that more biodiesel is consumed by the engine when compared with diesel to produce specific work at the same load and speed. It can be said that this property is one of the disadvantages of using biodiesel in internal combustion engines, which all types of biofuels from all feedstocks have in common.[40,42,45,52,59]

Table 2. Fuel Used in the Recent Study Features

fuel analysis	diesel (ULSD)	biodiesel (RME)
chemical formula	$C_{14}H_{26.18}$	$C_{18.96}H_{35.29}O_2$
cetane number	53.9	54.7
density at 15 °C (kg/m^3)	827.1	881.5
viscosity at 40 °C (cSt)	2.47	4.48
flash point (°C)	49	53
boiling point (°C)	278	242
self-ignition temperature (°C)	214	218
lower calorific value (MJ/kg)	43.4	37.5
sulfur content (mg/kg)	≥46	≥5
aromatics (wt %)	24.3	
C (wt %)	86.44	77.10
H (wt %)	13.56	12.05
O (wt %)	0	10.85

2.2. Test Engine. Figure 1 shows a schematic diagram of the experimental setup used in the recent study while Figure 1b shows a photo of this setup. A naturally aspirated diesel engine type Ford Duratorq (Puma) is used in the tests. This engine consists of four cylinders with a volume of 2.0 L, and each cylinder contains four valves. A Schenck eddy current dynamometer is attached to the engine' flywheel. Table 3 illustrates the basic engine's features.

The combustion chamber pressure is measured during operation employing a pressure transducer (type Kistler) installed in the engine cylinder. LabView is used to record the signal from the pressure transducer. Cylinder pressure data is collected for every 100 revolutions of the crankshaft. The fuel injection system is a common rail, and the injector has six injector holes (0.154 mm diameter per hole, and a spray angle of 154°). An electronic control unit that uses Gredi software is attached to the injection system. Brake fuel consumption is measured employing the AVL fuel economy gauge. This scale is based on the principle of gravity.

2.3. Regulated and Unregulated Emissions Measurement. A Horiba-Mexa 7170DEGR gas analyzer was used for engine regulated exhaust gas analysis under various engine operating conditions. Non-dispersive infrared technology (NDIR) was used to measure CO and CO_2 concentrations. NO_X emissions levels were measured using the chemiluminescence technique. The flame ionization detection technique

https://doi.org/10.1021/acsomega.2c00893
ACS Omega 2022, 7, 26056−26075

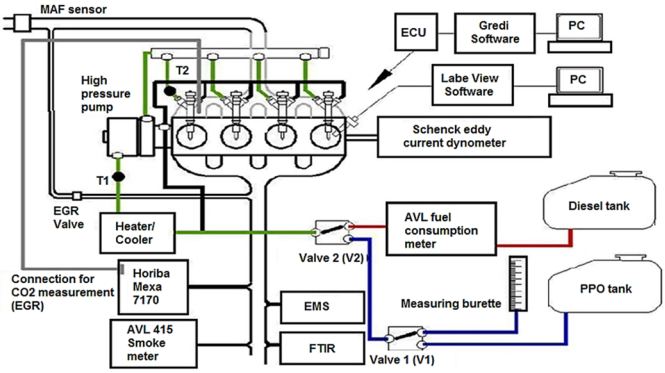

a. Schematic diagram of the engine and it facilities

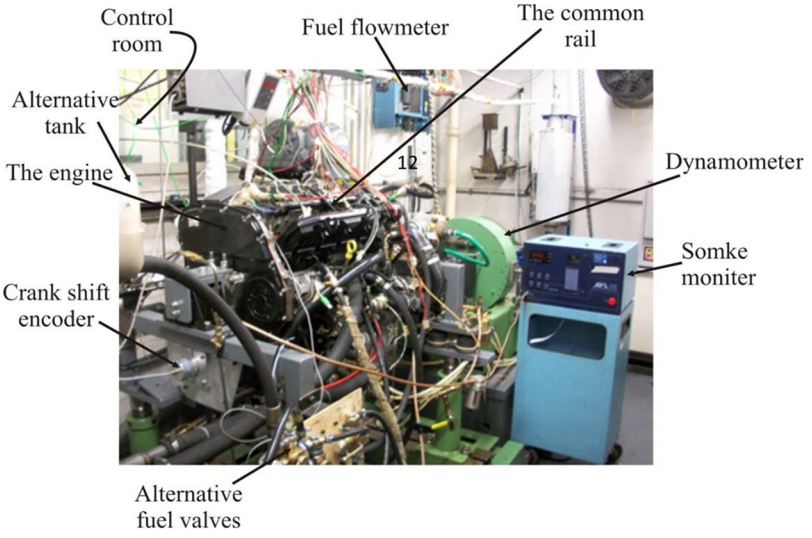

b. A photo of the engine

Figure 1. (a) Schematic diagram of the engine and its facilities.(b) Photo of the engine.

Table 3. Specifications of the 4-Cylinder Naturally Aspirated Diesel Engine Used in the Experiments

displacement (cm^3)	1998.23
compression ratio	18.2:1
bore (cm)	8.6
stroke (cm)	8.6
connecting rod length (cm)	15.5
cylinder pressure in bar (maximum)	150
piston form	central bowl inside the piston
maximum power at 1500 rpm (kW)	600
maximum torque (Nm)	100 (6.5 bar BMEP)
maximum no load speed (rpm)	4800 ± 50 rpm
idle engine speed (rpm)	750 ± 5 rpm
cooling water temperature (°C)	75

was employed to measure HC concentrations. An AVL-415 smoke meter was used in measuring the smoke emitted. A multigas 2030 FTIR spectrometer (Fourier transform infrared spectrometry) was employed to measure the unregulated emissions. Both units were equipped and installed by MKS Instruments UK, Ltd. Soot particles size distribution in the exhaust gases was measured using an electrostatic motion spectroscope (EMS). Both units were calibrated before starting the test every day.

2.4. Combustion Analysis. In this study, a heat release model used LabView software to download the pressure data in the combustion chamber to MATLAP and process it. The treatment is done by extracting the peak pressure, peak pressure angle, combustion onset, and apparent heat release rate (AHRR), without a specific heat transfer model.[74] The total heat release rate is the loss due to a large part of this heat being excreted with the exhaust in addition to the other part moving through the cylinder walls. Equation 1 shows the AHRR, which is derived from the first law of thermodynamics and the energy balance equations in the combustion chamber.

$$\delta Q_{ch} = \mathrm{d}U_s + \delta Q_{ht} + \delta W + \sum h_i \mathrm{d}m_i \tag{1}$$

Equation 1 has been simplified to

$$\frac{\mathrm{d}Q_{ch}}{\mathrm{d}\theta} = \frac{\gamma}{\gamma - 1} p \frac{\mathrm{d}V}{\mathrm{d}\theta} + \frac{1}{\gamma - 1} V \frac{\mathrm{d}p}{\mathrm{d}\theta} + V_{cr} \frac{\mathrm{d}p}{\mathrm{d}\theta} + \frac{\mathrm{d}Q_{ht}}{\mathrm{d}\theta} \tag{2}$$

Also, this formula can be reformulated without correcting the heat loss from inside the combustion chamber through the cylinder walls:

$$\frac{\mathrm{d}Q_{cha}}{\mathrm{d}\theta} = \frac{\gamma}{\gamma - 1} p \frac{\mathrm{d}V}{\mathrm{d}\theta} + \frac{1}{\gamma - 1} V \frac{\mathrm{d}p}{\mathrm{d}\theta} \tag{3}$$

https://doi.org/10.1021/acsomega.2c00893
ACS Omega 2022, 7, 26056−26075

Equations 1 and 2 were used to calculate the AHRR, and these two equations show a reasonable change in the energy applied to the piston. Previous studies explained in detail how temperature at certain limits clearly affects the formation of the peak heat release rate inside the combustion chamber.[75,76] Peirce et al.[77] indicated that the constant temperature is usually between 1.3 and 1.35. In the current study, two different types of fuel will be used under various engine operating conditions; therefore, the constant temperature = 1.35 was adopted according to what was directed by ref 77. The AHRR can be considered as the sum of the net heat of release rates at each crank angle (CAD), which was calculated from the start of the injection and is represented by the following relationship:

$$\mathrm{AHRR} = \sum_{\mathrm{SOI}}^{\mathrm{CAD}=720} \frac{\mathrm{d}Q_{ch}(i)}{\mathrm{d}\theta\ (i)}.\ k(i) \tag{4}$$

Figure 2 shows a schematic description of the AHRR parameters. The data were controlled so that one medium

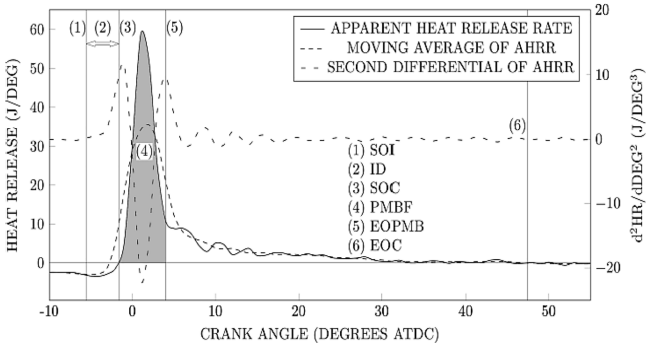

Figure 2. Schematic description of the AHRR parameters.

pressure generation could be described by specifying a data set of 100 pressure cycles. This procedure reduces noise in results and preserves combustion properties. With exception of the combustion end region, the AHRR curve calculations were neither filtered nor averaged. As for the end-of-combustion zone, the arithmetic mean was used to enhance the consistency.

bsfc is defined using the following relationship:

$$\mathrm{bsfc} = \frac{\dot{m}_f}{P} \tag{5}$$

2.5. Uncertainty Analysis. The accuracy of the results depends on the extent to which the measured values agree with the true values, and the measurement error is expressed by the amount of inaccuracy. Accuracy represents the degree of reliability of measurements and results. It expresses the uncertainty in the measurement differences due to several factors that affect the accuracy of the measurement. The great difference between the concepts of accuracy in measurement and uncertainty must be underscored. In empirical studies, uncertainty analyses are used to quantitatively demonstrate accuracy. The uncertainty value is expressed by the addition and subtraction signs, and the signs indicate that the measured value is higher or lower than the expected value by the amount following the two signs. In empirical studies, uncertainty is analyzed to ensure that the measurements are within the acceptable range assuming that the accuracy is close to an ideal value. Uncertainty is directly related to measurement errors, whether they are random or systematic. The method of Klein and McClintock[78] for uncertainty estimation was adopted in the current study. In this method, tests are used to determine the various experimental measurement errors using the following equation:

$$W_R = \left[\left(\frac{\partial R}{\partial x_1}w_1\right)^2 + \left(\frac{\partial R}{\partial x_2}w_2\right)^2 + \cdots + \left(\frac{\partial R}{\partial x_n}w_n\right)^2\right]^{0.5} \tag{6}$$

W_R is the results' uncertainty, R represents an independent variable function $(x_1, x_2, \ldots, x_n)$, and $(w_1, w_2, \ldots, w_n)$ expresses the independent variables' uncertainties. In this study, the uncertainty in measurements of the engine's performance and combustion characteristics (listed in Table 4) was

$$W_{R_1} = [(0.012)^2 + (0.18)^2 + (0.1)^2 + (0.9)^2 + (0.19)^2 + (0.22)^2]^{0.5} = 1.776 \tag{7}$$

The emitted pollutant measurement uncertainty (listed in Table 5) was

$$W_{R_2} = [(0.15)^2 + (0.50)^2 + (0.50)^2 + (0.045)^2 + (0.34)^2 + (0.30)^2 + (0.11)^2 + (0.44)^2 + (0.12)^2 + (0.27)^2 + (0.14)^2 + (0.28)^2]^{0.5} = 1.0588 \tag{8}$$

The test total uncertainty is

$$W_{R_1} = [(1.776)^2 + (1.0588)^2]^{0.5} = 2.067 \tag{9}$$

This result (uncertainty < 3%) indicates high measuring accuracy.

2.6. Test Procedure. The combustion characteristics of the two fuels used during this study were evaluated using the single injection method, and during all experiments, the concentrations of regulated and unregulated emitted pollutants were measured. The pressure transducer prepares pressure measurements inside the cylinder and sends this data to the LabView program that analyzes it. Program results initialize AHRR, burning time, ignition delay, start of combustion, and bsfc.

Table 4. Uncertainties of Engine Performance and Combustion Characteristics of the Measuring Instruments

instrument	measured parameter	measurement limit	accuracy (%)	experimental uncertainty (%)
dynamometer	engine torque	0−100 Nm	−1.43	±1.12
pressure transducer	combustion chamber pressure	0−250 bar	−3.40	±0.18
AVL fuel gauge	fuel consumption	125 kg/h	+1.2	±0.1
entering air gauge	air consumption	6.89 bar	+0.77	±0.9
thermocouples	temperature (inlet air, outlet exhaust gas, and ambient)	−200 to 2500 °C	−2.3	±0.19
flow meter	fuel flow rate (kg/s)	1.44 kg/s	−0.83	±0.52

https://doi.org/10.1021/acsomega.2c00893
ACS Omega 2022, 7, 26056−26075

Table 5. Measured Emissions and Their Uncertainty

pollutant	measurements limit (ppm)	instrument	accuracy (%)	uncertainty (%)
		Regulated emissions		
CO	0−745	Horiba-Mexa 7170DEGR gas analyzer	+0.78	± 0.15
HC	0−280	Horiba-Mexa 7170DEGR gas analyzer	−0.56	± 0.50
NOx	7−4100	Horiba-Mexa 7170DEGR gas analyzer	−1.14	± 0.50
smoke	0−1	AVL-415 smoke meter	−0.34	±0.045
		Unregulated emissions		
C_2H_4O (acetaldehyde)	0−135	multigas 2030 FTIR spectrometer	+1.2	± 0.30
C_2H_4O (acetone)	0−935	multigas 2030 FTIR spectrometer	−0.044	± 0.11
C_2H_2 (acetylene)	0−465	multigas 2030 FTIR spectrometer	−0.56	± 0.44
C_2H_4 (ethylene)	0−300	multigas 2030 FTIR spectrometer	−0.087	± 0.12
CH_2O (formaldehyde)	0−70	multigas 2030 FTIR spectrometer	−0.60	± 0.27
CH_4 (methane)	0−465	multigas 2030 FTIR spectrometer	+0.45	± 0.14
C_3H_6 (propylene)	0−125	multigas 2030 FTIR spectrometer	+0.62	± 0.28

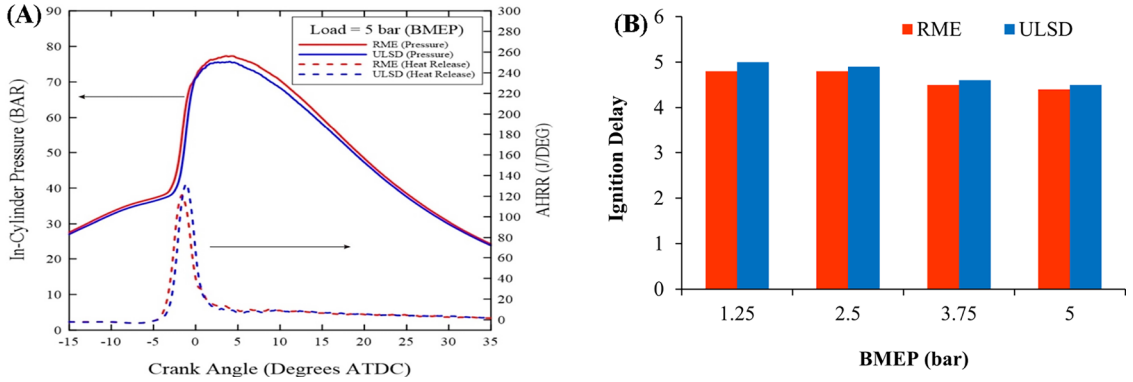

Figure 3. (A) In-cylinder pressure and heat release and (B) ignition delay.

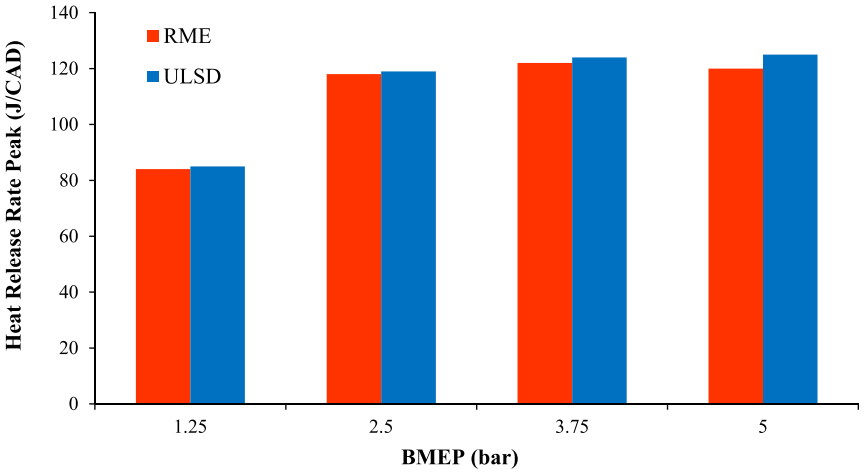

Figure 4. Peak of heat release rate at variable engine loads.

There are many conditions in which the engine can be tested. To eliminate these conditions, the engine has a rotation speed of 1500 rpm and it was loaded with four loads, which are 1.25, 2.5, 3.75, and 5 bar. These conditions may not fully represent the engine's combustion features, but rather the operating conditions of an engine on city roads. The engine design optimum injection angle (9° bTDC) was used in the first set of trials to be the reference in comparison for both fuels. Practical experiments have been completed in the Center for Advanced Powertrain and Fuel Research (CAPF), College of Engineering and Design, Brunel University (United Kingdom). The test conditions inside the laboratory were set at an air temperature of 25 °C, air pressure of 1 bar at sea level, and relative humidity of 35%.

3. RESULTS AND DISCUSSION

3.1. Combustion Characteristics. Figure 3A manifests the change in combustion chamber pressure and the released temperature with the crank angle change under high load [5 bar brake mean effective pressure (BMEP)] engine operating conditions and engine's optimum injection timing (OIT) of 9° bTDC for ULSD and RME. The RME combustion chamber pressure curve increased ahead of the same curve for the ULSD utilization case. These results are confirmed by the

https://doi.org/10.1021/acsomega.2c00893
ACS Omega 2022, 7, 26056−26075

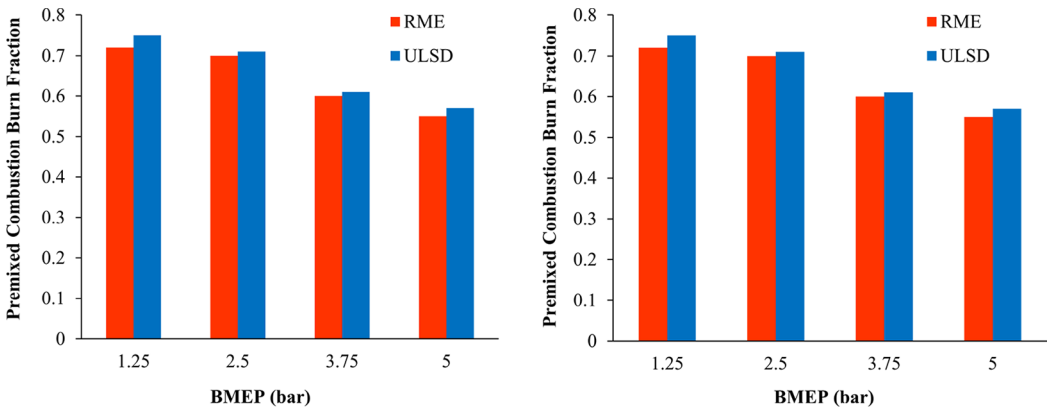

Figure 5. Pre-mixed and diffusion burn fraction at variable engine loads.

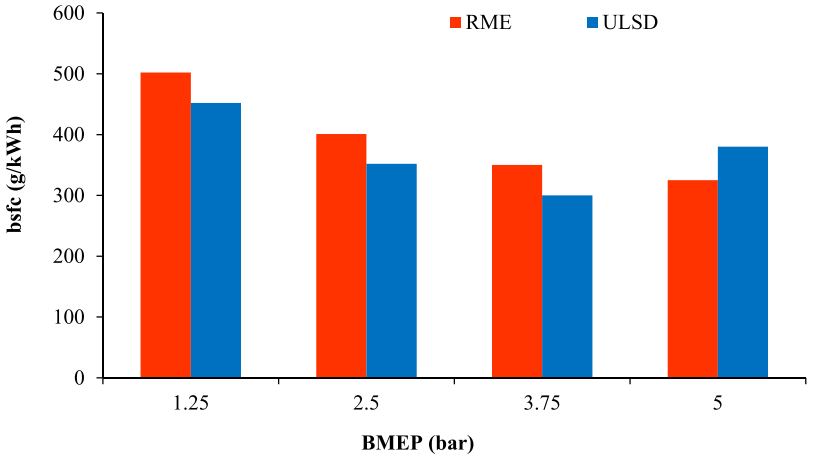

Figure 6. bsfc variation at studied engine loads.

similarly oriented AHRR curves. Figure 3B shows that the RME ignition delay period (IDP) is always shorter than that of ULSD fuel. These results can be traced back to the physicochemical properties of the RME fuel such as high cetane number and low vapor pressure. The IDP is highly dependent on the cetane number of the fuel.[79,80] Additionally, increasing the combustion temperature in the cylinder enhances the self-ignition of the fuel, which reduces this period at medium and high loads. The results indicate that the ignition delay period decreased with the increase in the load of the two fuels due to the increase in cylinder pressure and temperature.[54]

Figure 4 shows the measured combustion chamber peak pressure, which was relatively higher when ULSD is used compared to RME, for all engine loads tested. The amount of injected fuel inside the cylinder increased when the engine is overloaded, in order to raise the energy required to an acceptable level that runs the engine at a certain speed with such a load. The increased energy released from the fuel causes an increase in the combustion chamber pressure. For the two tested fuels, the highest peak HRR was at high loads (Figure 4). HRR was higher for diesel than for RME for all the studied loads. The HRR increment rates were 2.3%, 1.66%, 2.4%, and 4% in favor of ULSD at 1.25, 2.5, 3.75, and 5 bar, respectively. The peak temperature of diesel can be traced back to its higher calorific value compared to that of RME.

Another explanation for this result can also be given as Figure 5 illustrates that ULSD has a longer IDP, which increases the quantity of fuel burned in the pre-mixing stage.[54] Although the pre-mixed combustion phase is short, the energy released during this period is higher than its counterparts in the diffusion phase. The combustion during the pre-mixed fuel stage is close to complete combustion due to the quality of the fuel−air mixing.[81] For RME, oxygen concentration plays a vital role in reducing pyrolysis and increasing the oxidation, causing the ignition delay period to become shorter than that of diesel. The AHRR increases with increasing injection pressure, increasing the heat of combustion released, and increasing the pre-mixing phase.[4,82] A higher AHRR means reduced CO and HC emissions and an increase in NO_X concentrations.[79] The results from Figure 5 show that with increasing engine loads, the pre-mixed combustion part decreases and the diffuse combustion part increases.

The bsfc of both tested fuels increased at low load engine operation, as shown in Figure 6. The bsfc increased as the engine load was decreased due to the incomplete combustion of the fuel resulting from the combustion chamber's low temperature. According to Figure 6, the results show that biodiesel bsfc had higher values than that of diesel, for all the tested loads. The fuel consumption increased by 9.4%, 12.5%, and 14.7% when the engine was running under engine loads of 1.25, 2.5, and 3.5 bar, respectively. It is reported that the bsfc increases when the engine was fed with biofuel including RME, and this can be brought back to its LHV in comparison with diesel (Table 1). These results are in agreement with a previous study by Fayad et al.[79] In the case of high load (5

https://doi.org/10.1021/acsomega.2c00893
ACS Omega 2022, 7, 26056−26075

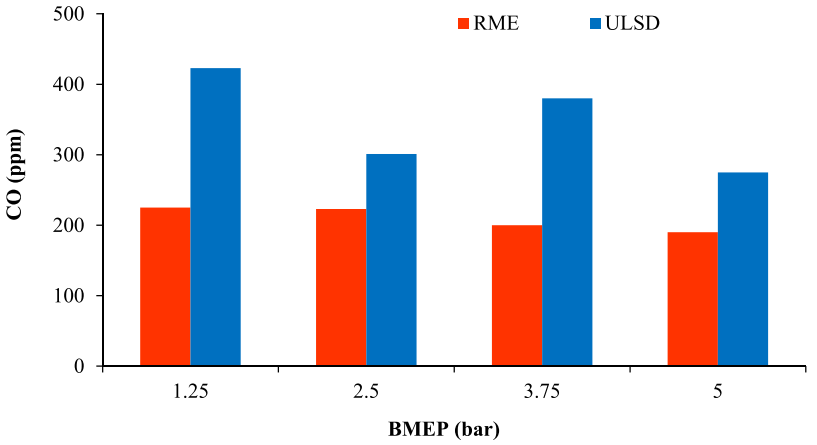

Figure 7. CO level variation at different loads (BMEP).

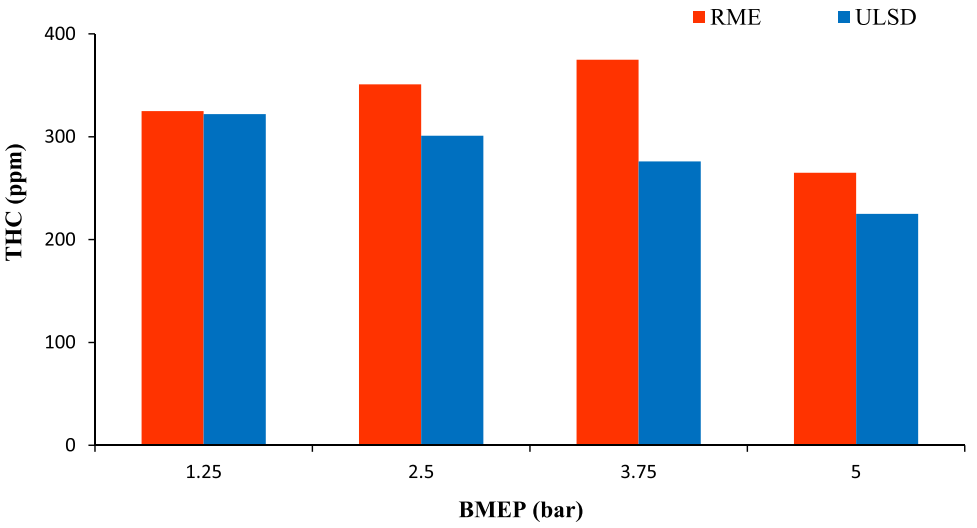

Figure 8. THC levels variation at studied loads.

bar), due to the higher temperature of the combustion chamber, the viscosity of RME was decreased, which led to lower consumption compared to diesel.[57]

3.2. Regulated Emissions. Carbon monoxide is formed during the combustion process as an intermediate oxidation stage of carbon and appears in the exhaust as a result of incomplete combustion. This pollutant is released in the local fuel-rich areas inside the combustion chamber. These areas are formed in terms of their density and distribution, depending on the pressure and angle of injection. CO is also formed as a result of the low temperature inside the combustion chamber, which inhibits oxidation reactions. The experimental results showed that CO concentrations decreased when the engine was fueled with RME at all load values studied, as shown in Figure 7. An increase in the load causes the high combustion temperatures inside the combustion chamber as well as the high fuel injected quantity. The CO concentrations reduced by 46.8, 25.9%, 47.36%, and 30.9% at 1.25, 2.5, 3.75, and 5 bar engine load, respectively. This outcome agrees with a previous study.[25]

The best control of CO levels is through the fuel equivalence ratio inside the cylinder. The oxidation process slows down under low temperature conditions inside the combustion chamber when the engine is running at low loads. Also, operating the engine at rich equivalence ratios with a decrease in the oxygen required for oxidation will cause high CO levels even under high engine load operating conditions. The oxygen molecule in the RME composition promotes the combustion of local rich mixtures reducing the CO concentrations emitted.

HC is formed inside the cylinders because of flame extinguishing on the cold cylinders' walls as well as the low combustion gas temperature inside the combustion chamber.[69] When the engine was fueled with RME and when the engine is overloaded, HC concentrations were noticed to be increased, as shown in Figure 8. The higher engine load causes the combustion chamber temperature to rise, which results in better oxidation reactions. The emergence of HC concentrations in the exhaust of the RME engine, which contains a high percentage of oxygen, can be traced back to the high viscosity of RME. This high viscosity causes spray penetration and delays fuel evaporation for a longer period and, in most cases when the combustion chamber temperature drops, wets the cylinder walls. This hydration produces high levels of HC.[9,27] The results showed that RME emitted a higher HC level approximately by 3.07% in comparison with ULSD at lower loads (1.25 bar), and these levels escalated to a peak (at engine load of 3.5 bar) with an increase rate of about 38.3%. Also, at high engine loads (5 bar), RME emitted higher HC concentrations of about 15% than ULSD. This result is consistent with the results of many studies, some of which are

https://doi.org/10.1021/acsomega.2c00893
ACS Omega 2022, 7, 26056−26075

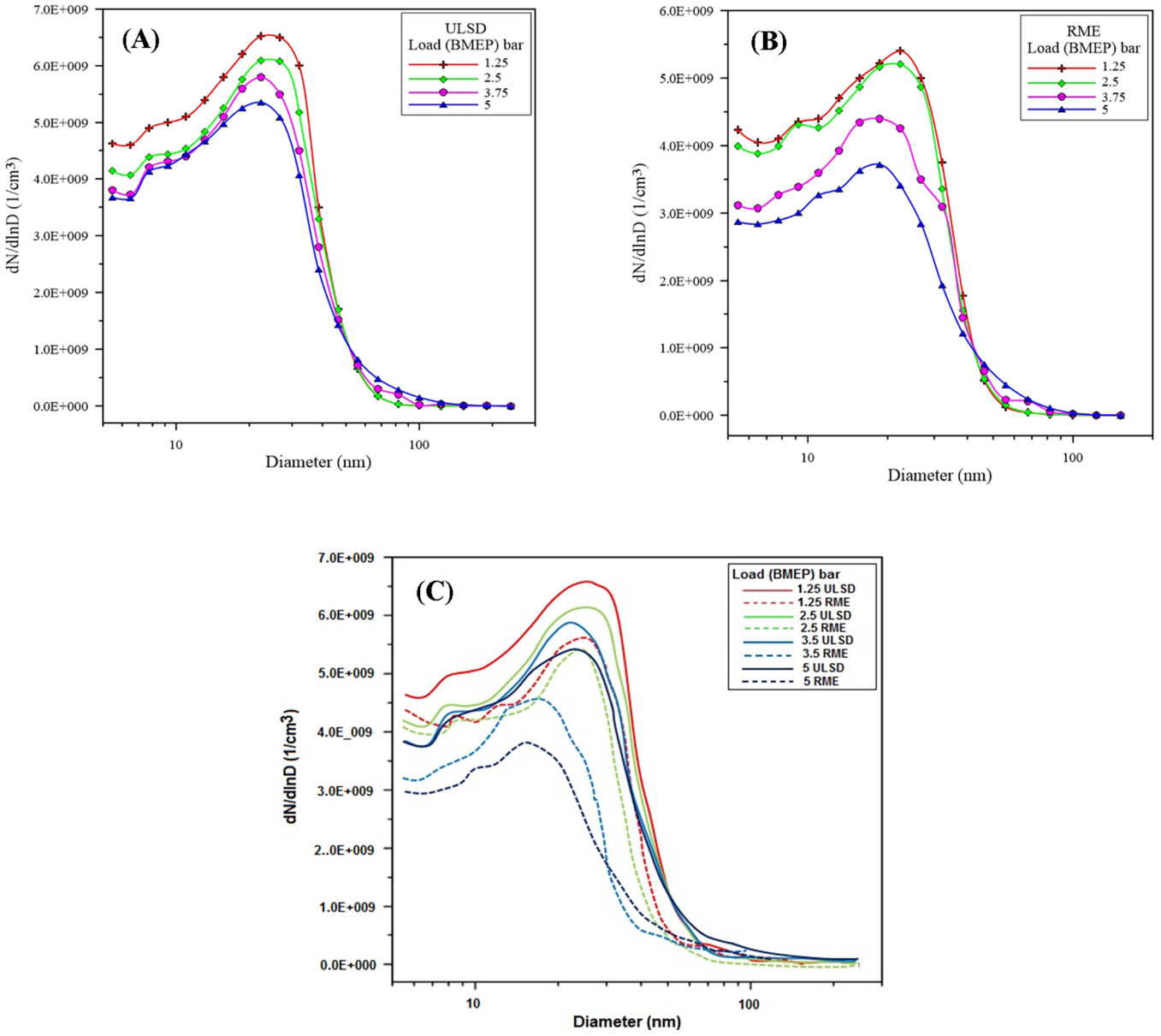

Figure 9. Load variation impact on particulate number levels and size distribution for (A) ULSD and (B) RME and (C) comparison between both fuels.

mentioned in Table 1.[36,38,41,45,56,63] Teoh et al.[56] showed that variation in HC emissions is not related to engine speed or load but to the combustion chamber and fuel injection system designs. Valente et al.[83] reported an increase in hydrocarbon concentrations with increased engine load as a direct result of combustion efficiency. The fuel/air mixture is enriched at high loads, which improves the combustion speed but provides an opportunity to extinguish the flame due to excessive cooling of the combustion chamber gases because of biodiesel vaporization. This result is consistent with previous studies,[84,85] which were carried out on stationary diesel engines as in the current study. However, most of the published studies were conducted on car engines using an electronic engine control unit that makes self-adjustments to reduce the concentrations of pollutants emitted according to the combustion conditions and the characteristics of the fuel used. In this study, the conditions for processing diesel fuel in the engine were adopted and the injection conditions were not changed when using biodiesel as fuel. Therefore, the differences in the design of the combustion chamber and the fuel injection system can be considered the reason for the difference in the results of these emissions from one study to another, up and down.

One of the most important pollutants emitted from engines is particulate matter (PM), which consists of groups of organic and inorganic compounds. The fuels' sulfur content plays an important role in the formation of PM.[86] Figure 9A shows the change in PM particle diameters as the engine load changes when fuelled with USLD, while Figure 9B shows this change when the engine is running on RME. Most of the particles emitted from the USLD engine have a particle diameter ranging between 5 and slightly larger than 100 nm. The diameter of these particles decreases when the engine load increases, to be confined to a range of diameter from 5 to 40 nm. This result confirms the decrease in the size of these particles, sub-micron, with an increase in load. When the engine runs at low loads, due to the large pre-mixed

https://doi.org/10.1021/acsomega.2c00893
ACS Omega 2022, 7, 26056−26075

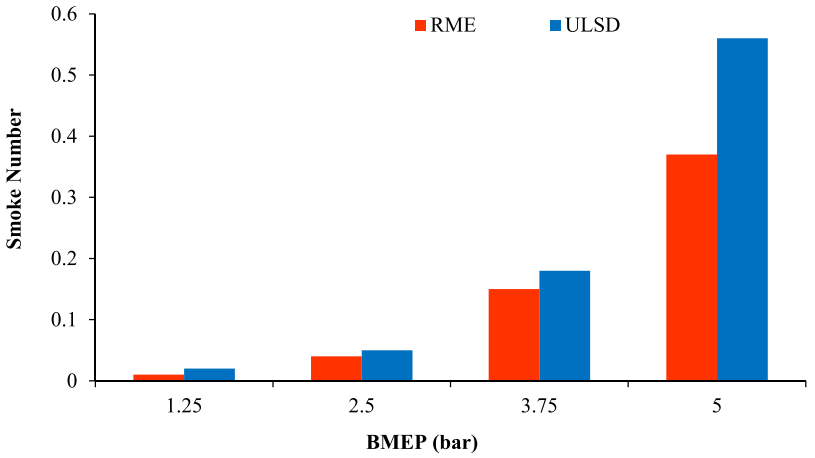

Figure 10. Engine load variation impact on emitted smoke number.

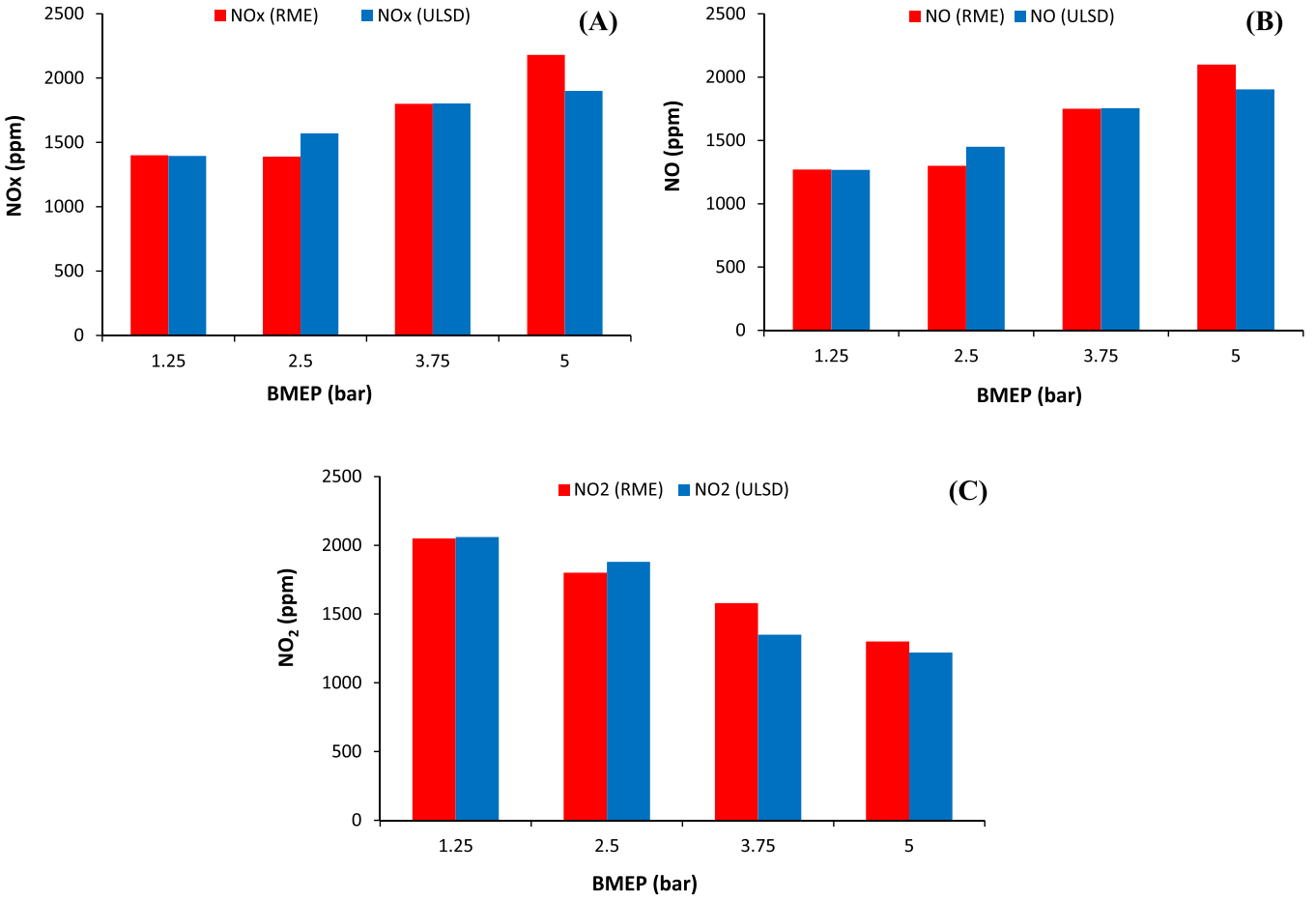

Figure 11. Engine load variation impact on NO_X, NO, and NO_2 levels.

combustion part, these conditions do not allow the small particles to coagulate and aggregate to form larger particles. In the event that the engine is operating at high loads, it consumes more fuel during the propagation period, which results in the formation of additional concentrations of PM, which helps in increasing the coagulation rate and forming a larger particle number with larger particle diameters.

All oxygenated fuels of various types, whether biological or industrial, emit fewer particles and have a smaller diameter compared to diesel. This is confirmed by Figure 9C that compares the emitted PM particle diameters for both studied fuels. Several factors cause a reduction in the average particle size, including an increase in the combustion temperature inside the cylinder, which reduces the formation rate of PM, as well as the suppression of particle collision that prevents the formation of larger particles. Larger particles are formed by particles clumping together as the combustion gases cool. A decrease in the particles' number and the agglomeration rate cause smaller particles to form with a decrease in the average particle diameter.[86,87]

The use of RME causes nanostructured particles with greater oxidative potential, which promotes increased combustion

https://doi.org/10.1021/acsomega.2c00893
ACS Omega 2022, 7, 26056−26075

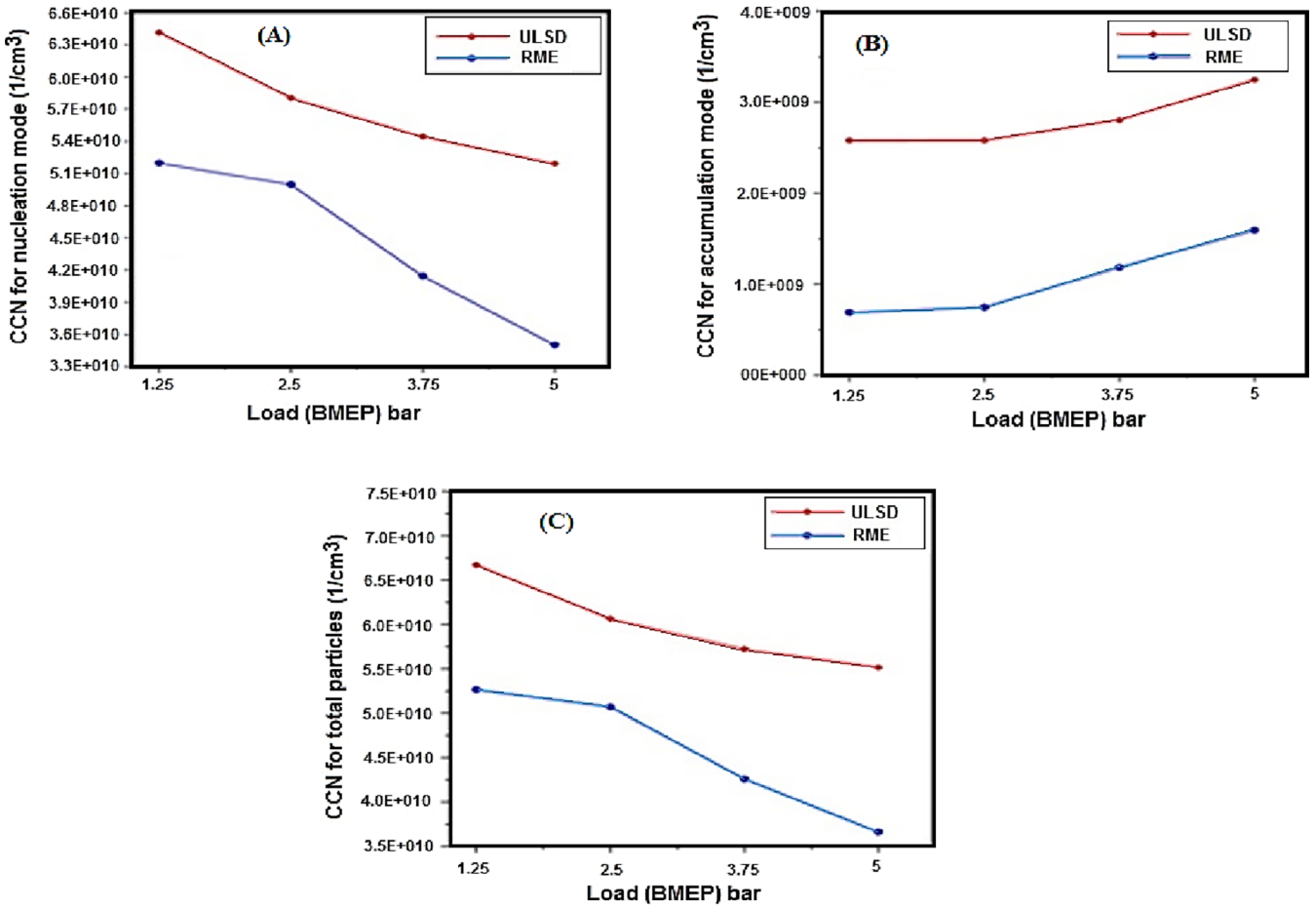

Figure 12. BMEP impact on CCN for nucleation mode (A), accumulation mode (B), and total PM concentration number (C).

compared to PM formed from ULSD combustion. At higher loads, where more fuel is injected, the air/fuel ratio and excess oxygen decrease with it in addition to the combustion chamber high pressure and temperature, and all of these factors contribute to the intolerance of PM as well as intended nucleation growth.[88] The higher oxygen content in RME improves combustion of locally rich equivalent ratios during the diffusion combustion fraction, resulting in reduced formation of particles with large diameters.[82]

The smoke number (SN) increased when the engine load was increased, and it was higher for the ULSD case as shown in Figure 10. The SN reduction rates from RME compared to that from diesel were 50%, 20%, 16.66%, and 33.9% for 1.25, 2.5, 3.75, and 5 bar, respectively. Smoke levels depend on several factors, including the equivalent ratio, the combustion temperatures inside the combustion chamber, and the good mixing of air and fuel. Local hypoxia in some locations of the combustion chamber causes high smoke concentrations.[59] RME emits less smoke compared to USLD, especially at higher engine loads. The difference in smoke number for the two tested fuels at low loads is limited. The large presence of oxygen in RME is the primary reason for reducing the smoke number. This oxygen helps oxidize the fuel and reduce the smoke formation in the diffusion combustion stage. Therefore, the smoke number for RME is clearly reduced when the engine is running at high loads since in this case, more fuel is burned during the diffusion mode.[60]

Another factor that can cause reduction in the smoke number is the low percentage of aromatics in RME as the formation of a large amount of smoke occurs in the diffusion burning mode. The pre-mixing state depends on the availability of hydrocarbons such as aromatics, alkenes, and alkanes.[89] In this situation too, the effect of the length of the hydrocarbon chain is clear on smoke formation.[90,91] Hence, the absence of aromatic substances from the chemical formula of RME had a positive effect on reducing the smoke number emitted from its engine.[50,51]

NO_X expresses a group of nitrogenous compounds like NO, NO_2, NH_3, etc., which result from the combustion process and emitted by the engine. For both RME and ULSD, the NO_X emission levels increased, as shown by the curves of Figure 11, with increasing engine load. The figure shows the changes in NO_X, NO, and NO_2 with the engine load. The NO_X concentration formed inside the combustion chamber depends mainly on the temperature and air/oxygen. Hence, increased load causes an increase in NO_X levels. For both fuels, NO_X levels are roughly equal at low load such as 1.25 bar.

This result is similar to what was achieved by Chen et al.[92] who observed relatively lower NO_X concentrations for biodiesel compared to diesel at lower loads for low and medium engine speeds (low or medium combustion chamber temperatures). The authors indicated that the reason for this decrease could be attributed to the high viscosity and negative effects of the distillation temperature on spray quality and the homogeneity of the air−fuel mixture at low loads and low and

https://doi.org/10.1021/acsomega.2c00893
ACS Omega 2022, 7, 26056−26075

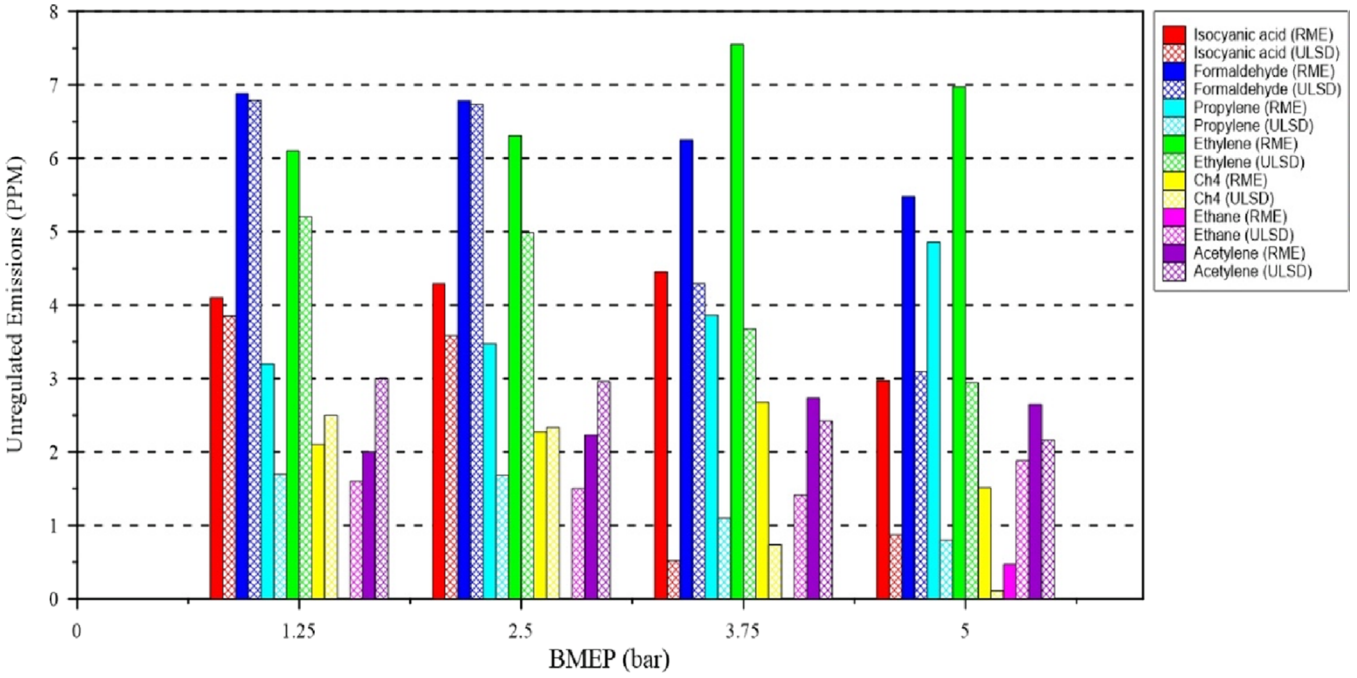

Figure 13. Impact of engine load variation on unregulated emissions for the tested fuels.

medium speeds. With increased engine load, NOx emissions from the RME engine outperformed those from a diesel engine. The increase in NOx emissions was 12% at an engine pressure of 2.5 bar in favor of diesel. Here, it is expected that the cooling effect of biodiesel evaporation reduced the temperature of the gases formed inside the combustion chamber, which hinders the NO_X formation. The NO_X levels for both fuels converged at 3.75 bar with a slight rise in RME. The highest emission difference achieved was 13% in favor of RME when carrying a 5 bar engine load (Figure 11). The main reason to justify this rise is the increase in the combustion chamber temperature and the increase of the amount of fresh air inside the combustion chamber as the engine load increased. Therefore, the high temperature of the combustion chamber promoted the formation of higher concentrations of NO_X.[93] When working with RME, the oxygen abundance and the high combustion temperature produced higher levels of NO_X. When working with ULSD, the ignition delay period for this fuel is longer and the pre-mixed combustion fraction is larger, which increases the combustion temperature, causing high NO_X levels for the low-load condition. Pearce et al.[94] confirmed that RME combustion emits lower NO_X levels compared to ULSD under the low-load conditions at the pre-mixed combustion fraction condition. However, the exact opposite happens at high loads. The researchers correlated these results for both fuels with variation in combustion duration, delay period, and pre-mixed combustion fraction. Also, in this study, the use of fixed ignition timings that suited with diesel combustion may be advanced for RME. As a result, higher levels of NO_X were emitted in the exhaust.[95]

3.3. Nanoparticle Size. Among the various suspended particles in the air, nanoparticles with diameters ranging from 1 to 100 nm are the most dangerous.[96] The time for these particles to remain suspended in the atmosphere is up to 1 week. While the coarse particles are removed from the atmosphere through their deposition, the smaller particles are not deposited for a period of time during which they are collected and agglomerated.[97] The long stay of particles of minute size in the atmospheric air poses many risks to human health as it is considered a carcinogen.[98] The time of human exposure to ultrafine particulate matter significantly increased, especially in indoor environments (homes and offices) in which most people spend their time.[99] Most of these nanoparticles are emitted by human activities such as exhaust from internal combustion engines, power plant chimneys, and industrial fires.[100]

Nanoparticles are formed due to incomplete combustion based on solid nucleation (sulfur particles help greatly in its formation), and their sizes differ due to heterogeneous and homogeneous nucleation during the formation process. The reasons for the homogeneity and heterogeneity are still unclear. Most of the nanoparticles are formed inside the cylinder in the fuel-rich region due to incomplete combustion resulting from its low temperature.[101,102]

Figure 12 shows the cumulative concentration number (CCN) during the nucleation and accumulation mode of the studied loads. Particles with diameters smaller than 40 nm represent the nucleation mode, while particles larger than this measure represent the accretion mode. Figure 12a shows that the CCN for the nucleation mode decreases with increasing load, while the CCN for the accumulation mode increases with increasing load (Figure 12b). At high loads, the accumulation of particles increases with the increase in the coagulation rate, and this situation results in an increase in the rate of larger diameter particle formation. From RME combustion, fewer particles are formed during the accretion mode (diameters greater than 40 nm).

The reason can be traced back to the abundance of oxygen in the RME formula, which enhances the combustion quality in the fraction of the flame spread out in the local rich equivalence ratio regions within the cylinder.[94] This enhancement increases the oxidation rate of the formed fine particles.[94] Also, the absence of aromatics in the RME formulation reduced the activated PM molecules during the accumulation

https://doi.org/10.1021/acsomega.2c00893
ACS Omega 2022, 7, 26056−26075

mode.[82] The result obtained (reduction of PM formation during the accumulation mode when the engine is running on RME) is consistent with the findings of refs 79, 103−105. When using RME, there was a decrease in the total number of particles (Figure 12c) when calculating the number of particles for the accumulation and nucleation method. The use of RME not only caused a decrease in PM but also caused the CCN of the total particles formed to increase.

3.4. Unregulated Pollutants. Measurements of the unregulated pollutant levels (in Figure 13) show very low values as most of these pollutants have a concentration of less than 8 ppm. The emitted aldehydes are intermediate products found in hydrocarbon or oxygenated fuels.[106] Formaldehyde (CH_2O) is the most commonly measured aldehyde in exhaust gases, and its concentration diminution with increasing engine load for both fuels was tested. Formaldehyde is also an intermediate combustion product, which results in the combustion chamber temperature's significant increase. The results show that the measured formaldehyde levels were increased when the engine was run on RME by 1.47%, 1.09%, 48.8%, and 74.8% for 1.25, 2.5, 3.75, and 5 bar, respectively, compared to the diesel. This result was confirmed by previous works.[107−110] The same references indicated that under low-load conditions, high levels of formaldehyde are also emitted (6.9 and 6.8 ppm at 1.25 and 2.5 bar). This means that formaldehyde is formed at low temperatures, and its formation is in areas where the air/fuel mixture is fat-free. Guarieiro et al.[111] mentioned that the relatively high concentration of formaldehyde is due to the presence of an amount of short-chain (saturated) methyl esters in biofuels that form the shorter chain carbonyls during combustion.

The curves of Figure 13 show that ethane (C_2H_6) does not change significantly with the change in the load of the used diesel, but when working with biodiesel, concentrations that can be measured only appear at engine loads above 5 bar. The levels of ethylene (C_2H_4), which results from the pyrolysis of both ULSD and RME, decreased. Ethylene is the simplest unsaturated alkene that can be considered after acetylene. Ethylene concentrations decreased when the engine was running on diesel fuel at high loads while when the engine was running on biodiesel, the ethylene concentration increased with increased load and reached its maximum values when the engine was loaded at 3.75 bar.

The behavior of the emitted propylene (C_3H_6) is similar to that of HC. It increases with an increase in engine load when working with RME and decreases when the engine is running on diesel. This behavior is due to the same reasons that explain the case of HC.[53] When RME fueled the engine, the C_3H_6 increment rates were 88.2%, 100%, 250%, and 506% for MBEP 1.25, 2.5, 3.75, and 5 bar, respectively, compared to ULSD. As for the unsaturated alkene (CH_4) and acetylene (C_2H_2), they have the same orientation. Ethylene, acetylene, and propylene are considered hazardous materials due to their high reactivity and toxicity. These substances are produced from pyrolysis, and then they react to form polycyclic aromatic hydrocarbons (PAHs), which are the nuclei of PAM molecules.[109,112,113] The levels of C_2H_4, C_2H_2, and C_3H_6 are affected by the equivalence ratio and temperature of combustion. At high load conditions, the high combustion chamber temperature oxidizes the pyrolysis products. In the same conditions, the rich equivalence ratio causes the pyrolysis products to rise. The increment rates for ethylene when RME was used were 26%, 47%, 105.47%, and 137.28% for engine BMEP of 1.25, 2.5, 3.75, and 5 bar, respectively, compared to ULSD. When RME was used, methane concentrations at 1.25 and 2.5 bar were less than those when ULSD was used by 16% and 4.3% while at 3.75 and 5 bar operation, its concentrations exceeded those when ULSD was used by 271.4% and 400%, respectively. Acetylene concentrations for RME started lower than that emitted by ULSD at 1.25 and 2.5 bar by 33.3% and 26.66%, respectively. When the loads increased to 3.75 and 5 bar, RME emitted higher levels of acetylene than ULSD by 17.39% and 30.23%, respectively.

Isocyanic acid (HNCO) is a simple and stable chemical compound composed of hydrogen, carbon, oxygen, and nitrogen atoms, which are the most common elements in organic chemistry. This acid is produced by reactions between H_2, NO, and CO. For ULSD, when the engine load is increased, the isocyanic acid concentrations were decreased (3.9, 3.5, 0.5, and 0.4 ppm for 1.25, 2.5, 3.75, and 5 bar, respectively). However, when biodiesel is used, the rise in isocyanic acid concentrations with load increasing was limited (4.1, 4.3, 5.5, and 3.0 ppm for 1.25, 2.5, 3.75, and 5 bar, respectively). An increase in the engine load leads to a significant increase in the temperature of the combustion chamber. This state increases the reaction rate of H, O, and N molecules, which reduces the formation of this acid.[62] In the case of using RME biofuel, there is more oxygen inside the combustion chamber, which helps to increase the relative formation of isocyanic acid.

4. CONCLUSIONS

RME is an environmentally friendly and green fuel that can operate compression ignition engines with very minor modifications to the engine design. In the current study, the combustion properties, the concentrations of regulated and unregulated pollutants, and the size of the nanoparticles emitted from the engine operation were tested using RME. The obtained results are compared to ULSD under the same engine operating conditions. The experimental results demonstrated that the AHRR of RME fuel is higher than that of ULSD, and the IDP was always shorter than the ULSD ones by 2 to 3 CAD. In addition, it was found that the diesel has a higher heat release rate than RME. The bsfc from RME combustion was higher than that from diesel by 9.4% at low loads and increased to 11.3% at high loads.

The exhaust gas emission results showed that CO emitted levels when the engine is running on RME were significantly lower than on ULSD by 46.3%, and this decrement retracted to 30.9% at high loads. HC concentrations increased when the engine was running on RME to reach a value about 38.3% higher than on ULSD at high load. Most of the output PM from a diesel engine has a particle size from 5 to 100 nm, while for the RME engine working condition, the particle size was from 5 to 40 nm. It was observed that the nanoparticle sizes decreased with the increase of engine load for both fuels. The smoke number for ULSD was higher than for RME, and this number increased with increasing load. The results also revealed that NO_X concentration was relatively high (13%) in the case of RME and in both fuels increased with increasing engine load. Measurements of formaldehyde, ethane, methane, acetylene, ethylene, propylene, and isocyanic acid emissions showed the presence of these harmful substances at very low concentrations (less than 8 ppm). At 5 bar BMEP, the formaldehyde, methane, acetylene, ethylene, propylene, and isocyanic acid concentrations were higher than for ULSD by

https://doi.org/10.1021/acsomega.2c00893
ACS Omega 2022, 7, 26056−26075

74.8%, 400%, 30.23%, 137.28%, 506%, and 650%, respectively. In conclusion, more investigations are needed to reduce unregulated pollutants as in the case of regulated emissions. Further studies should be conducted on RME using EGR, post-process catalysts, and particulate filters, which will be the future work.

AUTHOR INFORMATION

Corresponding Authors

Miqdam T Chaichan − *Energy and Renewable Energies Technology Center, University of Technology-Iraq, Baghdad 10001, Iraq*; Email: miqdam.t.chaichan@uotechnology.edu.iq

Ahmed Al-Amiery − *Energy and Renewable Energies Technology Center, University of Technology-Iraq, Baghdad 10001, Iraq; Department of Chemical and Process Engineering, Faculty of Engineering and Built Environment, Universiti Kebangsaan Malaysia (UKM), Bangi 43600 Selangor, Malaysia;* orcid.org/0000-0003-1033-4904; Email: dr.ahmed1975@ukm.edu.my, 100173@uotechnology.edu.iq

Authors

Mohammed A. Fayad − *Energy and Renewable Energies Technology Center, University of Technology-Iraq, Baghdad 10001, Iraq*

Amged Al Ezzi − *Electromechanical Engineering Department, University of Technology-Iraq, Baghdad 10001, Iraq*

Hayder A Dhahad − *Mechanical Engineering Department, University of Technology-Iraq, Baghdad 10001, Iraq*

T. Megaritis − *Centre for Advanced Powertrain and Fuels Research School of Engineering and Design, Brunel University, London UB8 3PH, UK*

Talal Yusaf − *Business Development Department, Aviation Australia, Brisbane 4004 QLD, Australia*

Wan Nor Roslam Wan Isahak − *Department of Chemical and Process Engineering, Faculty of Engineering and Built Environment, Universiti Kebangsaan Malaysia (UKM), Bangi 43600 Selangor, Malaysia;* orcid.org/0000-0002-1051-3120

Complete contact information is available at: https://pubs.acs.org/10.1021/acsomega.2c00893

Notes

The authors declare no competing financial interest.

NOMENCLATURE

bsfc brake specific fuel combustion
EOC end of combustion
EOPMB end of pre-mixed burn
Hidmi losses by the crevices
ID ignition delay
k resolution of the heat release rate expressed in 1/measured point in 0.125 CAD
m°_{f} fuel mass flow rate
P engine output power
p in-cylinder pressure
PMBF pre-mixed burn fraction
OIT optimum injection timing
Q_{ht} convective heat transfer to the cylinder walls
SOC start of combustion
SOI start of injection
Us internal energy
V cylinder volume
W work output
γ adiabatic index (specific heats ratio)
θ crank angle degree

REFERENCES

(1) Yilmaz, N.; Atmanli, A. Experimental evaluation of a diesel engine running on the blends of diesel and pentanol as a next generation higher alcohol. *Fuel* **2017**, *210*, 75−82.

(2) IEA. *World energy outlook International Energy Agency*; 2009.

(3) Sakthivel, G. Prediction of CI engine performance, emission and combustion characteristics using fish oil as a biodiesel at different injection timing using fuzzy logic. *Fuel* **2016**, *183*, 214−229.

(4) Dhahad, H. A.; Chaichan, M. T.; Megaritis, T. Performance, regulated and unregulated exhaust emission of a stationary compression ignition engine fueled by water-ULSD emulsion. *Energy* **2019**, *181*, 1036−1050.

(5) Chaichan, M. T.; Kazem, H. A.; Abed, T. A. Traffic and outdoor air pollution levels near highways in Baghdad, Iraq. *Environ. Dev. Sustainability* **2018**, *20*, 589−603.

(6) Fayad, M. A. Investigating the influence of oxygenated fuel on particulate size distribution and NO_X control in a common-rail diesel engine at rated EGR levels. *Therm. Sci. Eng. Prog.* **2020**, *19*, No. 100621.

(7) Hamza, N. H.; Ekaab, N. S.; Chaichan, M. T. The impact of using Iraqi biofuel-kerosene blends on coarse and fine particulate matter emitted from compression ignition engines. *Alexandria Eng. J.* **2020**, *59*, 1717−1724.

(8) US EPA. *Health Assessment Document for Diesel Engine Exhaust, National Center for Environmental Assessment, Office of Transportation and Air Quality*; US Environmental Protection Agency, EPA/600/8−90/057F, 2002.

(9) Ekaab, N. S.; Hamza, N. H.; Chaichan, M. T. Performance and emitted pollutants assessment of diesel engine fuelled with Biokerosene. *Case Stud. Therm. Eng.* **2019**, *13*, No. 100381.

(10) Shah, S. D.; Cocker, D. R.; Miller, J. W.; Norbeck, J. M. Emission rates of particulate matter and elemental and organic carbon from in-use diesel engines. *Environ. Sci. Technol.* **2004**, *38*, 2544−2550.

(11) Fayad, M. A.; Herreros, J. M.; Martos, F. J.; Tsolakis, A. Role of alternative fuels on particulate matter (PM) characteristics and influence of the diesel oxidation catalyst. *Environ. Sci. Technol.* **2015**, *49*, 11967−11973.

(12) Sahoo, B. B.; Sahoo, N.; Saha, U. K. Effect of engine parameters and type of gaseous fuel on the performance of dual-fuel gas diesel engines-A critical review. *Renewable Sustainable Energy Rev.* **2009**, *13*, 1151−1184.

(13) Houidi, M. B.; AlRamadan, A. S.; Sotton, J.; Bellenoue, M.; Sarathy, S. M.; Johansson, B. Understanding multi-stage HCCI combustion caused by thermal stratification and chemical three-stage auto-ignition. *Proc. Combust. Inst.* **2021**, *38*, 5575−5583.

(14) Liang, X.; Zhang, J.; Li, Z.; Zhang, J.; Huang, Z.; Han, D. Effects of fuel combination and IVO timing on combustion and emissions of a dual-fuel HCCI combustion engine. *Front. Energy* **2020**, *14*, 778−789.

(15) Dhahad, H. A.; Fayad, M. A.; Chaichan, M. T.; Jaber, A. A.; Megaritis, T. Influence of fuel injection timing strategies on performance, combustion, emissions and particulate matter characteristics fueled with rapeseed methyl ester in modern diesel engine. *Fuel* **2021**, *306*, No. 121589.

(16) Wang, X.; Wang, M.; Han, Y.; Chen, H. Identifying unregulated emissions from conventional diesel self-ignition and PPCI marine engines at full load conditions. *J. Mar. Sci. Eng.* **2020**, *8*, 101.

(17) Leach, F. C. P.; Davy, M.; Terry, B. Combustion and emissions from cerium oxide nanoparticle dosed diesel fuel in a high speed diesel research engine under low temperature combustion (LTC) conditions. *Fuel* **2021**, *288*, No. 119636.

(18) Chaudhari, V. D.; Deshmukh, D. Diesel and diesel-gasoline fuelled premixed low temperature combustion (LTC) engine mode for clean combustion. *Fuel* **2020**, *266*, No. 116982.
(19) Dhahad, H. A.; Ali, S. A.; Chaichan, M. T. Combustion analysis and performance characteristics of compression ignition engines with diesel fuel supplemented with nano-TiO2 and nano-Al2O3. *Case Stud. Therm. Eng.* **2020**, *20*, No. 100651.
(20) Dhahad, H. A.; Chaichan, M. T. The impact of adding nano-Al_2O_3 and nano-ZnO to Iraqi diesel fuel in terms of compression ignition engines' performance and emitted pollutants. *Therm. Sci. Eng. Prog.* **2020**, *18*, No. 100535.
(21) Lapuerta, M.; Armas, O.; Jose, R. F. Effect of biodiesel fuels on diesel engine emissions. *Prog. Energy Combust. Sci.* **2008**, *34*, 198−223.
(22) Chaichan, M. T.; Kadhum, A. H.; Al-Amiery, A. A. Novel technique for enhancement of diesel fuel: Impact of aqueous alumina nano-fluid on engine's performance and emissions. *Case Stud. Therm. Eng.* **2017**, *10*, 611−620.
(23) Fayad, M. A.; Dhahad, H. A. Effects of adding aluminum oxide nanoparticles to butanol-diesel blends on performance, particulate matter, and emission characteristics of diesel engine. *Fuel* **2021**, *286*, No. 119363.
(24) Devarajana, Y.; Beemkumarb, N.; Ganesanc, S.; Arunkumar, T. An experimental study on the influence of an oxygenated additive in diesel engine fuelled with neat papaya seed biodiesel/diesel blends. *Fuel* **2020**, *268*, No. 117254.
(25) Wang, Z.; Qi, Y.; He, X.; Wang, J.; Shuai, S.; Law, C. K. Analysis of pre-ignition to super-knock: Hotspot-induced deflagration to detonation. *Fuel* **2015**, *144*, 222−227.
(26) Fayad, M. A. Effect of renewable fuel and injection strategies on combustion characteristics and gaseous emissions in diesel engines. *Energy Sources, Part A* **2020**, *42*, 460−470.
(27) Qi, D. H.; Geng, L. M.; Chen, H.; Bian, Y. Z. H.; Liu, J.; Ren, X. C. H. Combustion and performance evaluation of a diesel engine fueled with biodiesel produced from soybean crude oil. *Renewable Energy* **2009**, *34*, 2706−2713.
(28) Sarin, A.; Arora, R.; Singh, N. P.; Sarin, R.; Malhotra, R. K.; Kundu, K. Effect of blends of Palm−Jatropha−Pongamia biodiesels on cloud point and pour point. *Energy* **2009**, *34*, 2016−2021.
(29) Knothe, G.; Steidley, K. R. Kinematic viscosity of biodiesel fuel components and related compounds, influence of compound structure and comparison to petro diesel fuel components. *Fuel* **2005**, *84*, 1059−1065.
(30) Bruno, T. J.; Wolk, A.; Naydich, A.; Huber, M. L. Composition-explicit distillation curves for mixtures of diesel fuel with dimethyl carbonate and diethyl carbonate. *Energy Fuels* **2009**, *23*, 3989−3997.
(31) Fayad, M. A.; Al-Salihi, H. A.; Dhahad, H. A.; Mohammed, F. M.; Al-Ogidi, B. R. Effect of post-injection and alternative fuels on combustion, emissions and soot nanoparticles characteristics in a common-rail direct injection diesel engine. *Energy Sources, Part A* **2021**, 1−15.
(32) He, C.; Ge, Y.; Tan, J.; You, K.; Han, X.; Wang, J.; You, Q.; Shah, A. N. Comparison of carbonyl compounds emissions from diesel engine fueled with biodiesel and diesel. *Atmos. Environ.* **2009**, *43*, 3657−3661.
(33) Sahoo, P. K.; Das, L. M.; Babu, M. K. G.; Arora, P.; Singh, V. P.; Kumar, N. R.; Varyani, T. S. Comparative evaluation of performance and emission characteristics of jatropha, karanja and polanga based biodiesel as fuel in a tractor engine. *Fuel* **2009**, *88*, 1698−1707.
(34) Fayad, M. A. Investigation the impact of injection timing and pressure on emissions characteristics and smoke/soot emissions in diesel engine fueling with soybean fuel. *J. Eng. Res.* **2021**, *9*, 296−307.
(35) Senthamaraikannan, P.; Sivaprakasam, S.; Saravanan, C.G. Combustion and emission analysis on DI diesel engine run on animal fat oil. In: *8th Asia Pacific conference on combustion (ASPACC 2010), India*. 2010, 1005−1009.
(36) Saravanan, C. G.; Kiran, K. R.; Vikneswaran, M.; Rajakrishnamoorthy, P.; Yadav, S. P. R. Impact of fuel injection pressure on the engine characteristics of CRDI engine powered by pine oil biodiesel blend. *Fuel* **2020**, *264*, No. 116760.
(37) Krishania, N.; Rajak, U.; Chaurasiya, P. K.; Singh, T. S.; Birru, A. K.; Verma, T. N. Investigations of spirulina, waste cooking and animal fats blended biodiesel fuel on auto-ignition diesel engine performance, emission characteristics. *Fuel* **2020**, *276*, No. 118123.
(38) Markiewicz, M.; Muślewski, Ł. Survey performance and emission parameters of diesel engine powered by diesel oil and fatty acid methyl esters using fuzzy logic techniques. *Fuel* **2020**, *277*, No. 118179.
(39) Kanth, S.; Debbarma, S. Comparative performance analysis of diesel engine fuelled with hydrogen enriched edible and non-edible biodiesel. *Int. J. Hydrogen Energy* **2021**, *46*, 10478−10493.
(40) Akcay, M.; Yilmaz, I. T.; Feyzioglu, A. Effect of hydrogen addition on performance and emission characteristics of a common-rail CI engine fueled with diesel/waste cooking oil biodiesel blends. *Energy* **2020**, *212*, No. 118538.
(41) Mikulski, M.; Ambrosewicz-Walacik, M.; Duda, K.; Hunicz, J. Performance and emission characterization of a common-rail compression-ignition engine fuelled with ternary mixtures of rapeseed oil, pyrolytic oil and diesel. *Renewable Energy* **2020**, *148*, 739−755.
(42) Venu, H.; Raju, V. D.; Subramani, L.; Appavu, P. Experimental assessment on the regulated and unregulated emissions of DI diesel engine fuelled with Chlorella emersonii methyl ester (CEME). *Renewable Energy* **2020**, *151*, 88−102.
(43) Dieng, M. T.; Iwanaga, T.; Yurie, Y. C.; Torii, S. Evaluation of performance and emission characteristics of biodiesel fuel produced from rapeseed oil. *J. Energy Power Eng.* **2020**, *14*, 75−84.
(44) Altaie, M. A. H.; Alhadithy, S. A.; Janius, R. B. Analysis of performance of engine and exhaust emissions with modified biodiesel fuel. *J. Innovations Energy Sci.* **2020**, *1*, 2.
(45) Atabani, A. E.; Kulthoom, S. A. Spectral, thermos-analytical characterizations, properties, engine and emission performance of complementary biodiesel-diesel-pentanol/octanol blends. *Fuel* **2020**, *282*, 118849.
(46) Kodate, S. V.; Raju, P. S.; Yadav, A. K.; Kumar, G. N. Investigation of preheated Dhupa seed oil biodiesel as an alternative fuel on the performance, emission and combustion in a CI engine. *Energy* **2021**, *231*, No. 120874.
(47) Khoobbakht, G.; Kheiralipour, K.; Karimi, M. Optimization of chlamydomonas alga biodiesel percentage for reducing exhaust emission of diesel engine. *Process Saf. Environ. Prot.* **2021**, *152*, 25−36.
(48) Ma, Q.; Zhang, Q.; Liang, J.; Yang, C. The performance and emissions characteristics of diesel/biodiesel/alcohol blends in a diesel engine. *Energy Rep.* **2021**, *7*, 1016−1024.
(49) Dębowski, M.; Michalski, R.; Zieliński, M.; Kazimierowicz, J. A comparative analysis of emissions from a compression−ignition engine powered by diesel, rapeseed biodiesel, and biodiesel from chlorella protothecoides biomass cultured under different conditions. *Atmosphere* **2021**, *12*, 1099.
(50) Čedík, J.; Pexa, M.; Holúbek, M.; Mrázek, J.; Valera, H.; Agarwal, A. K. Operational parameters of a diesel engine running on diesel−rapeseed oil−methanol iso-butanol blends. *Energies* **2021**, *14*, 6173.
(51) Rayapureddy, S. M.; Matijošius, J.; Rimkus, A. Comparison of research data of diesel−biodiesel−isopropanol and diesel−rapeseed oil−isopropanol fuel blends mixed at different proportions on a CI engine. *Sustainability* **2021**, *13*, 10059.
(52) Balasubramanian, D.; Hoang, A. T.; Venugopal, I. P.; Shanmugam, A.; Gao, J.; Wongwuttanasatian, T. Numerical and experimental evaluation on the pooled effect of waste cooking oil biodiesel/diesel blends and exhaust gas recirculation in a twin-cylinder diesel engine. *Fuel* **2021**, *287*, No. 119815.
(53) Puškár, M.; Živčák, J.; Král, Š.; Kopas, M.; Lavčák, M. Analysis of biodiesel influence on unregulated gaseous emissions of diesel motor vehicles. *Appl. Sci.* **2021**, *11*, 4646.
(54) Hadhoum, L.; Aklouche, F. Z.; Loubar, K.; Tazerout, M. Experimental investigation of performance, emission and combustion

https://doi.org/10.1021/acsomega.2c00893
ACS Omega 2022, 7, 26056−26075

characteristics of olive mill wastewater biofuel blends fuelled CI engine. *Fuel* **2021**, *291*, No. 120199.
(55) Yage, D.; Junjie, Z.; Shun, C. C.; Xuelong, M.; Jinbao, Z.; Haiyong, P.; Tao, W. Comparative study on combustion and particulate emissions for diesel-biodiesel and diesel-diglyme blends. *Fuel* **2022**, *313*, No. 122710.
(56) Teoh, Y. H.; Yaqoob, H.; How, H. G.; Le, T. D.; Nguyen, H. T. Comparative assessment of performance, emissions and combustion characteristics of tire pyrolysis oil-diesel and biodiesel-diesel blends in a common-rail direct injection engine. *Fuel* **2022**, *313*, No. 123058.
(57) Kodate, S. V.; Raju, P. S.; Yadav, A. K.; Kumar, G. N. Effect of fuel preheating on performance, emission and combustion characteristics of a diesel engine fuelled with Vateria indica methyl ester blends at various loads. *J. Environ. Manage.* **2022**, *304*, No. 114284.
(58) Zuo, L.; Wang, J.; Mei, D.; Dai, S.; Adu-Mensah, D. Experimental investigation on combustion and (regulated and unregulated) emissions performance of a common-rail diesel engine using partially hydrogenated biodiesel-ethanol-diesel ternary blend. *Renewable Energy* **2022**, *185*, 1272−1283.
(59) Jamshaid, M.; Masjuki, H. H.; Kalam, M. A.; Zulkifli, N. W. M.; Arslan, A.; Qureshi, A. A. Experimental investigation of performance, emissions and tribological characteristics of B20 blend from cottonseed and palm oil biodiesels. *Energy* **2022**, *239*, No. 121894.
(60) Jacob, A.; Ashok, B.; Usman, K. M.; Raja, V. B.; Jino, L. Synergistic effect of post injection and CART unit in extenuating Tail-Pipe pollutants in CI engine using C. pyrenoidosa microalgae biodiesel. *Sustainable Energy Technol. Assess.* **2022**, *52*, No. 102188.
(61) Niyas, M. M.; Saija, A. *Effect of repeated heating of coconut, sunflower, and palm oils on their fatty acid profiles, biodiesel properties and performance, combustion, and emission, characteristics of a diesel engine fueled with their biodiesel blends*. DOI: 10.2139/ssrn.4050292
(62) Agarwal, A. K.; Valera, H.; Mustafi, N. N. Di-ethyl ether-diesel blends fuelled off-road tractor engine: Part-II: Unregulated and particulate emission characteristics. *Fuel* **2022**, *308*, No. 121973.
(63) Chen, H.; Cheng, Y.; He, Q.; Wang, X. Experimental study on combustion and unregulated emission characteristics of a diesel engine fueled with light hydrocarbon/diesel blends. *Fuel* **2022**, *315*, No. 123075.
(64) Teoh, Y. H.; How, H. G.; Lee, S. W.; Loo, D. L.; Le, T. D.; Nguyen, H. T.; Sher, F. Optimization of engine out responses with different biodiesel fuel blends for energy transition. *Fuel* **2022**, *318*, No. 123706.
(65) Rajesh Kumar, B.; Saravanan, S. Partially premixed low temperature combustion using dimethyl carbonate (DMC) in a DI diesel engine for favorable smoke/NOx emissions. *Fuel* **2016**, *180*, 396−406.
(66) Fayad, M. A.; AL-Ogaidi, B. R.; Abood, M. K.; AL-Salihi, H. A. Influence of post-injection strategies and CeO_2 nanoparticles additives in the C30D blends and diesel on engine performance, NO_x emissions, and PM characteristics in diesel engine. *Part. Sci. Technol.* **2021**, 1−14.
(67) Zhang, J.; Jing, W.; Roberts, W. L.; Fang, T. Soot measurements for diesel and biodiesel spray combustion under high temperature highly diluted ambient conditions. *Fuel* **2014**, *135*, 340−351.
(68) Moniru, I. M.; Masjuki, H. H.; Kalam, M. A.; Mosarof, M. H.; Zulkifli, N. W. M.; Teoh, Y. H.; How, H. G. Assessment of performance, emission and combustion characteristics of palm, jatropha and Calophyllum inophyllum biodiesel blends. *Fuel* **2016**, *181*, 985−995.
(69) Chaichan, M. T. Performance and emissions characteristics of CIE using hydrogen, biodiesel, and massive EGR. *Int. J. Hydrogen Energy* **2018**, *43*, 5415−5435.
(70) Naresh Kumar, A.; Kishore, P. S.; Brahma Raju, K.; Nanthagopal, K.; Ashok, B. Experimental study on engine parameters variation in CRDI engine fuelled with palm biodiesel. *Fuel* **2020**, *276*, No. 118076.
(71) Karthic, S. V.; Senthil Kumar, M.; Nataraj, G.; Pradeep, P. An assessment on injection pressure and timing to reduce emissions on diesel engine powered by renewable fuel. *J. Cleaner Prod.* **2020**, *255*, No. 120186.
(72) Ashok, B.; Nanthagopal, K.; Saravanan, B.; Somasundaram, P.; Jegadheesan, C.; Chaturvedi, B.; Sharma, S.; Patni, G. A novel study on the effect lemon peel oil as a fuel in CRDI engine at various injection strategies. *Energy Convers. Manage.* **2018**, *172*, 517−528.
(73) Heywood, J. B.. *Internal combustion engine fundamentals*; McGraw-Hill Science Engineering, 1988.
(74) Lanzafame, R.; Messina, M. ICE gross heat release strongly influenced by specific heat ratio values. *Int. J. Automot. Technol.* **2003**, *4*, 125−133.
(75) Horn, U.; Egnell, R.; Johansson, B.; Andersson, Ö. *Detailed heat release analyses with regard to combustion of RME and oxygenated fuels in an HSDI diesel engine. SAE Technical Paper No. 2007-01-0627*. 2007.
(76) Christodoulou, F.; Megaritis, A. The effect of reformer gas mixture on the performance and emissions of an HSDI diesel engine. *Int. J. Hydrogen Energy* **2014**, *39*, 9798−9808.
(77) Peirce, D. M.; Alozie, N. S.; Hatherill, D. W.; Ganippa, L. C. Premixed burn fraction: its relation to the variation in NOx emissions between petro-and biodiesel. *Energy Fuels* **2013**, *27*, 3838−3852.
(78) Kline, S. J.; McClintock, F. A. Describing uncertainties in single-sample experiments. *Mech. Eng.* **1953**, 3−8.
(79) Fayad, M. A.; Tsolakis, A.; Fernández-Rodríguez, D.; Herreros, J. M.; Martos, F. J.; Lapuerta, M. Manipulating modern diesel engine particulate emission characteristics through butanol fuel blending and fuel injection strategies for efficient diesel oxidation catalysts. *Appl. Energy* **2017**, *190*, 490−500.
(80) Szybist, J. P., Boehman, A. L. *Behavior of a diesel injection system with biodiesel fuel. SAE Paper No. (2003−01−1039)*. 2003.
(81) Nour, M.; Attia, A. M.; Nada, S. A. Combustion, performance and emission analysis of diesel engine fuelled by higher alcohols (butanol, octanol and heptanol)/diesel blends. *Energy Convers. Manage.* **2019**, *185*, 313−329.
(82) Tsolakis, A. Effects on particle size distribution from the diesel engine operating on RME-biodiesel with EGR. *Energy Fuels* **2006**, *20*, 1418−1424.
(83) Valente, O. S.; Silva, M. J.; Pasa, V. M. D.; Belchior, C. R. P.; Sodre, J. R. Fuel consumption and emissions from a diesel power generator fuelled with castor oil and soybean biodiesel. *Fuel* **2010**, *89*, 3637−3642.
(84) Cetinkaya, M.; Karaosmanoğlu, F. A new application area for used cooking oil originated biodiesel: generators. *Energy Fuels* **2005**, *19*, 645−652.
(85) Pereira, R. G.; Oliveira, C. D.; Oliveira, J. L.; Oliveira, P. C. P.; Fellows, C. E.; Piamba, O. E. Exhaust emissions and electric energy generation in a stationary engine using blends of diesel and soybean biodiesel. *Renewable Energy* **2007**, *32*, 2453−2460.
(86) Tinsdale, M.; Price, P.; Chen, R. *The impact of biodiesel on particle number, size and mass emissions from a euro4 diesel vehicle. SAE Paper 2010-01-0796*, 2010.
(87) Tan, P. Q.; Hu, Z. Y.; Deng, K. Y.; Lu, J. X.; Lou, D. M.; Wan, G. Particulate matter emission modelling based on soot and SOF from direct injection diesel engines. *Energy Convers. Manage.* **2007**, *48*, 510−518.
(88) Dhahad, H. A.; Fayad, M. Role of different antioxidants additions to renewable fuels on NOx emissions reduction and smoke number in direct injection diesel engine. *Fuel* **2020**, *279*, No. 118384.
(89) Ladommatos, N.; Rubenstein, P.; Bennett, P. Some effects of molecular structure of single hydrocarbons on sooting tendency. *Fuel* **1996**, *75*, 114−124.
(90) Glassman, I. Soot formation in combustion processes. *Symp. (Int.) Combust.* **1988**, *22*, 295−311.
(91) Eastwood, P. *Particulate Emissions from Vehicles*; John Wiley and Sons Ltd.: Chichester, U.K., 2008.
(92) Chen, H.; Xie, B.; Ma, J.; Chen, Y. NO_x emission of biodiesel compared to diesel: Higher or lower? *Appl. Therm. Eng.* **2018**, *137*, 584−593.
(93) Chen, H.; He, J.; Chen, Z.; Geng, L. A comparative study of combustion and emission characteristics of dual-fuel engine fueled

with diesel/methanol and diesel−polyoxymethylene dimethyl ether blend/methanol. *Process Saf. Environ. Prot.* **2021**, *147*, 714−722.
(94) Peirce, D. M.; Alozie, N. S. I.; Hatherill, D. W.; Ganippa, L. C. Premixed burn fraction: Its relation to the variation in NO_x emissions between petro- and biodiesel. *Energy Fuels* **2013**, *27*, 3838−3852.
(95) Hoang, A. T. Combustion behavior, performance and emission characteristics of diesel engine fuelled with biodiesel containing cerium oxide nanoparticles: A review. *Fuel Process. Technol.* **2021**, *218*, No. 106840.
(96) Sonwani, S.; Madaan, S.; Arora, J.; Suryanarayan, S.; Rangra, D.; Mongia, N.; Vats, T.; Saxena, P. Inhalation exposure to atmospheric nanoparticles and its associated impacts on human health: A review. *Front. Sustainable Cities* **2021**, *3*, No. 690444.
(97) Bakshi, S.; He, Z. L.; Harris, W. G. Natural nanoparticles: implications for environment and human health. *Crit. Rev. Environ. Sci. Technol.* **2015**, *45*, 861−904.
(98) Banerjee, T.; Christian, R. A. A review on nanoparticle dispersion from vehicular exhaust: Assessment of Indian urban environment. *Atmos. Pollut. Res.* **2018**, *9*, 342−357.
(99) Ali, M. U.; Lin, S.; Yousaf, B.; Abbas, Q.; Munir, M. A. M.; Rashid, A.; Zheng, C.; Kuang, X.; Wong, M. H. Pollution characteristics, mechanism of toxicity and health effects of the ultrafine particles in the indoor environment: Current status and future perspectives. *Crit. Rev. Environ. Sci. Technol.* **2022**, *52*, 436−473.
(100) Jeevanandam, J.; Barhoum, A.; Chan, Y. S.; Dufresne, A.; Danquah, M. K. Review on nanoparticles and nanostructured materials: history, sources, toxicity and regulations. *Beilstein J. Nanotechnol.* **2018**, *9*, 1050−1074.
(101) Yusuf, A. A.; Inambao, F. L. Effect of cold start emissions from gasoline-fueled engines of light-duty vehicles at low and high ambient temperatures: Recent trends. *Case Stud. Therm. Eng.* **2019**, *14*, No. 100417.
(102) Chaichan, M.; Gaaz, T. S.; Al-Amiery, A.; Kadhum, A. A. Biodiesel blends startability and emissions during cold, warm and hot conditions. *J. Nanofluids* **2020**, *9*, 75−89.
(103) Jung, H.; Kittelson, D. B.; Zachariah, M. R. Characteristics of SME biodiesel-fueled diesel particle emissions and the kinetics of oxidation. *Environ. Sci. Technol.* **2006**, *40*, 4949−4955.
(104) Di, Y.; Cheung, C. S.; Huang, Z. Experimental investigation on regulated and unregulated emissions of a diesel engine fueled with ultra-low sulfur diesel fuel blended with biodiesel from waste cooking oil. *Sci. Total Environ.* **2009**, *407*, 835−846.
(105) Cheng, C. H.; Cheung, C. S.; Chan, T. L.; Lee, S. C.; Yao, C. D.; Tsang, K. S. Comparison of emissions of a direct injection diesel engine operating on biodiesel with emulsified and fumigated methanol. *Fuel* **2008**, *87*, 1870−1879.
(106) Takada, K.; Yoshimura, F.; Ohga, Y.; Kusaka, J.; Daisho, Y.; *Experimental Study on Unregulated Emission Characteristics of Turbo-charged Di Diesel Engine with Common Rail Fuel Injection System. SAE. 2003-01-3158.* 2003.
(107) Tan, P.; Hu, Z.; Lou, D.; Li, Z. Exhaust emissions from a light-duty diesel engine with Jatropha biodiesel fuel. *Energy* **2012**, *39*, 356−362.
(108) Fontaras, G.; Karavalakis, G.; Kousoulidou, M.; Ntziachristos, L.; Bakeas, E.; Stournas, S.; Samaras, Z. Effects of low concentration biodiesel blends application on modern passenger cars. Part 2: Impact on carbonyl compound emissions. *Environ. Pollut.* **2010**, *158*, 2496−2503.
(109) Zhu, R.; Cheung, C. S.; Huang, Z.; Wang, X. Regulated and unregulated emissions from a diesel engine fueled with diesel fuel blended with diethyl adipate. *Atmos. Environ.* **2011**, *45*, 2174−2181.
(110) Fayad, M. A.; Radhi, A. A.; Omran, S. H.; Mohammed, F. M. Influence of environment-friendly fuel additives and fuel injection pressure on soot nanoparticles characteristics and engine performance, and nox emissions in CI Diesel Engine. *J. Adv. Res. Fluid Mech. Therm. Sci.* **2021**, *88*, 58−70.
(111) Guarieiro, L. L. N.; Pereira, P. A. d. P.; Torres, E. A.; Rocha, G. O.; de Andrade, J. B. Carbonyl compounds emitted by a diesel engine fuelled with diesel and bio- diesel-diesel blends: sampling optimization and emissions profile. *Atmos. Environ.* **2008**, *42*, 8211−8218.
(112) Flynn, P. F.; Durrett, R. P.; Hunter, G. L.; Loye, A. O.; Akinyemi, O. C. *Diesel combustion: An integrated view combining laser diagnostics, chemical kinetics, and empirical validation. SAE paper 1999-01-0509*, 1999.
(113) Slude, C. S.; Wagner, R. M. *An estimate of diesel high-efficiency clean combustion impacts on FTP-75 after treatment requirements. SAE paper 2006-01-3311*, 2006.

https://doi.org/10.1021/acsomega.2c00893
ACS Omega 2022, 7, 26056−26075